

**BED SEDIMENT-TRACE ELEMENT GEOCHEMISTRY OF
TERRACE RESERVOIR, NEAR SUMMITVILLE,
SOUTHWESTERN, COLORADO**

By Arthur J. Horowitz, John A. Robbins, Kent A. Elrick, and Robert B. Cook

U.S. Geological Survey

Open-File Report 96-344



**Prepared in Cooperation with the
U.S. Environmental Protection Agency**

Atlanta, Georgia

1996

U. S. DEPARTMENT OF THE INTERIOR

BRUCE BABBITT, Secretary

U. S. Geological Survey

Gordon P. Eaton, Director

Any use of trade, product, or firm names is for descriptive purposes only and does not constitute an endorsement by the U.S. Government.

For additional information write to:

District Chief
U.S. Geological Survey
Peachtree Business Center
Suite 130, 3039 Amwiler Road
Atlanta, GA 30360-2824

Copies of this report can be purchased from:

U.S. Geological Survey
Branch of Information Services
Denver Federal Center
Box 25286
Denver, CO 80225-0286

CONTENTS

Abstract	1
Introduction	2
Purpose	3
Methods of investigation	3
Sample pretreatment	3
Analytical techniques	5
Geochemical partitioning	5
Radiometric dating measurements	5
¹³⁷ Cs and ⁴⁰ K determinations	6
²¹⁰ Pb determinations	6
Geochemistry of bed sediments	6
Bulk sediment chemistry	7
Chemical comparisons with sediments from the Alamosa River	9
Chemical comparisons of reservoir sediments with sediments from other areas	9
Trace element interrelations	13
Geochemical partitioning	13
Sediment-geochemical history of Terrace Reservoir	20
Effects of heap-leach mining activities	25
Conclusions	29
Selected references	29
Appendix 1 - Bulk chemical data for all the Terrace Reservoir study sediment samples	32
Appendix 2 - ¹³⁷ Cs geochronology	38
Appendix 3 - ²¹⁰ Pb geochronology	41

ILLUSTRATIONS

Figure	1.	General location map of the Summitville area	2
	2.	Detailed map of Terrace Reservoir	4
	3.	Selected plots of correlation coefficients	16
	4.	Graphical presentation of geochemical partitioning of light sediment fractions	21
	5.	The distribution of ¹³⁷ Cs activities with depth in three cores (V-3, C-3, and V-4)	22
	6.	The distribution of ¹³⁷ Cs with depth for core V-4 compared with a calculated distribution	24
	7.	The distribution of total and extracted ²¹⁰ Pb and ²²⁶ Ra in core V-4	26
	8.	The distribution of excess ²¹⁰ Pb plotted against a calculated exponential decay curve	27
A2.1		The upper graph (A) shows changes in the idealized ¹³⁷ Cs loading, with time to Terrace Reservoir, whereas the lower graph (B) shows a ¹³⁷ Cs sedimentary profile assuming the delivery of the idealized ¹³⁷ Cs loading depicted in the upper graph	40

TABLES

Table	1.	Minimum, maximum, mean, and median element concentrations for bed sediments from in and around Terrace Reservoir	8
	2.	Comparison of trace element concentrations in Terrace Reservoir sediments with those from nearby streams	10
	3.	Comparison of trace element concentrations in Terrace Reservoir sediments with those from other trace element-rich areas	11
	4.	Correlation coefficients for Terrace Reservoir and related sediments	14
	5.	Geochemical partitioning of selected sediment samples from Terrace Reservoir	17
	6.	Minimum, maximum, mean, and median concentrations for core samples deposited before and after the beginning of heap-leach mining operations	28

CONVERSION FACTORS AND ABBREVIATIONS

CONVERSION FACTORS

Multiply	by	to obtain
<i>Length</i>		
inch (in.)	25.4	millimeter
foot (ft.)	0.3048	meter
mile (mi)	1.609	kilometer
cubic foot per second (ft ³ s ⁻¹)	0.2832	cubic meter per second

Volume

gallon (gal)	0.003785	cubic meter
	3.785	liter

Temperature

Temperature, in degrees Fahrenheit (^oF), can be converted to degrees Celsius (^oC) as follows:

$$^{\circ}\text{C} = (^{\circ}\text{F} - 32) / 1.8$$

ABBREVIATIONS

Chemical Elements

<u>Symbol</u>	<u>Name</u>
Ag	silver
Al	aluminum
As	arsenic
Cd	cadmium
Co	cobalt
Cr	chromium
Cu	copper
Fe	iron
Hg	mercury
Mn	manganese
Ni	nickel
Pb	lead
Sb	antimony
TC	total carbon
Ti	titanium
Zn	zinc
⁴⁰ K	potassium (atomic mass = 40)
¹³⁷ Cs	caesium (atomic mass = 137)
²¹⁰ Pb	lead (atomic mass = 210)
²¹⁰ Po	polonium (atomic mass = 210)
²¹⁴ Bi	bismuth (atomic mass = 214)
²²² Rn	radon (atomic mass = 222)
²²⁶ Ra	radium (atomic mass = 226)
²³⁸ U	uranium (atomic mass = 238)
Carb	carbon
CO ₂	carbon dioxide
HCl	hydrochloric acid
HClO ₄	perchloric acid
HF	hydrofluoric acid
HpGe	high purity germanium
KI	potassium iodide
NH ₂ OH·HCl	hydroxylamine hydrochloride
Sulf	sulfur

Volume

μl	microliter
ml	milliliter
cc	cubic centimeter (ml)
l	liter

Length

μm	micrometer
cm	centimeter
m	meter
km	kilometer

ABBREVIATIONS—Continued

Mass

mg	milligram
g	gram
kg	kilogram

Density

g cc ⁻¹	grams per cubic centimeter
--------------------	----------------------------

Time

sec	second
min	minute
h	hour
d	day
wk	week
y	year
t _{1/2}	half-life

Concentration

ppm	parts-per-million
mg/kg	milligrams-per-kilogram (ppm)
dpm	disintegrations-per-minute
wt %	weight percent (10,000 ppm)

Voltage

KeV	thousands of electron volts
-----	-----------------------------

Analytical Instrumentation

ICP-AES	inductively coupled plasma atomic emission spectroscopy
AAS	atomic absorption spectrophotometry

BED SEDIMENT-TRACE ELEMENT GEOCHEMISTRY OF TERRACE RESERVOIR, NEAR SUMMITVILLE, SOUTHWESTERN, COLORADO

by

Arthur J. Horowitz¹, John A. Robbins², Kent A. Elrick¹, and Robert B. Cook³

ABSTRACT

In 1994, the U.S. Geological Survey conducted an extensive bed sediment geochemical survey in Terrace Reservoir, near Summitville, southwestern, Colorado. Both the surface (grab) and near-surface (core) sediments are substantially enriched in Cu, Pb, Zn, Cd, As, Sb, Hg, Fe, and Al relative to unaffected fine-grained sediments collected in a variety of environments throughout the United States. The majority of the enriched trace elements appear to be associated with operationally defined residual phases which are not likely to be environmentally available. The exceptions are Cu and Zn, which appear to be associated with operationally defined labile phases. Sediment-associated Cu, Pb, Zn, As, and Sb apparently are being exported downstream from the reservoir, into the San Luis Valley, by the Alamosa River. Attempts to develop a sediment-geochemical history of the reservoir using ¹³⁷Cs and ²¹⁰Pb indicate that the onset of trace element enrichment substantially predates the onset of heap-leach mining operations at Summitville. There are some indications, based on median and maximum sediment-associated trace element levels, that the onset of heap-leach mining may have marginally increased the concentrations and fluxes of some of the already enriched trace elements in the reservoir bed sediments.

¹U.S. Geological Survey, Suite 130, 3039 Amwiler Road, Atlanta, GA 30360.

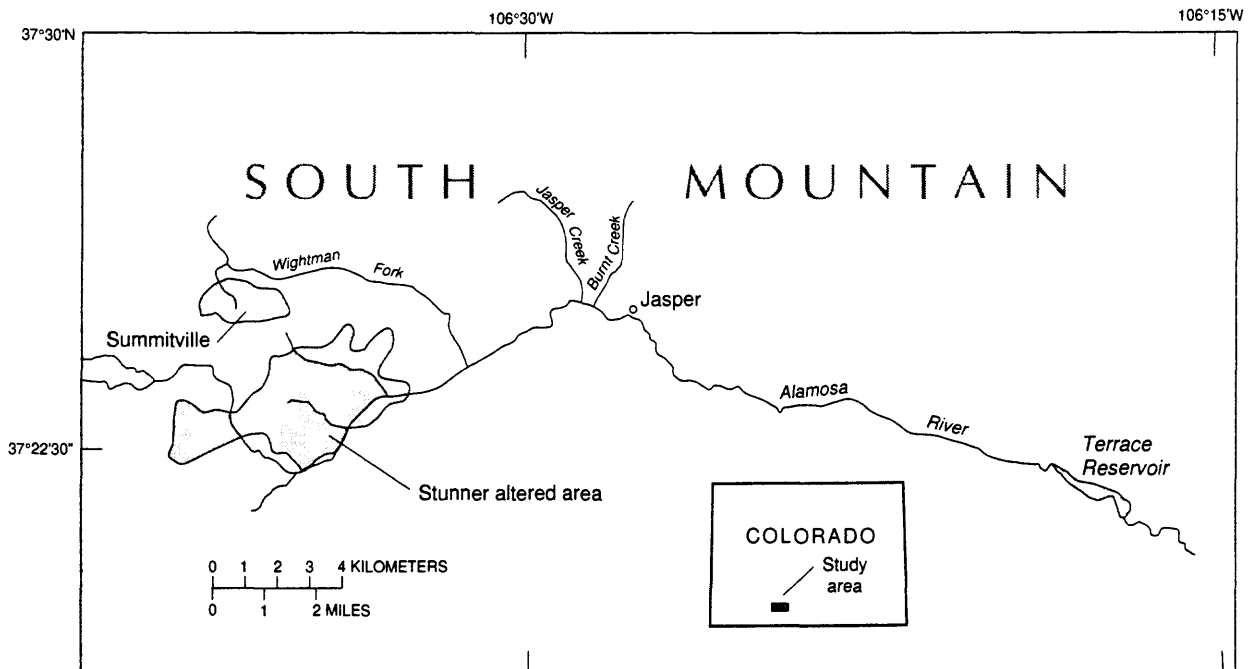
²National Oceanic and Atmospheric Administration, Great Lakes Environmental Research Laboratory, 2205 Commonwealth Blvd., Ann Arbor, MI 48103.

³Department of Geology, 210 Petrie Hall, Auburn University, Auburn, AL 36849.

INTRODUCTION

Gold initially was discovered in the Summitville District of Colorado around 1870 when placer deposits were found in stream gravels. Significant mining began on South Mountain in 1875, and continued intermittently into the late 1940's (Steven and Ratte, 1960). Initially, the ore was recovered by open-cut surface mining; however, after 1887, the majority was mined from underground workings. Silver was recovered along with the gold, and beginning in 1896, substantial amounts of copper and lead also were produced (Steven and Ratte, 1960). Maximum production occurred between 1875-1887, 1926-1928 and 1935-1943, whereas little or no ore was recovered between 1917-1923, 1930-1935, and after 1948 through the mid 1980's (Steven and Ratte, 1960; Pendleton, and others, 1995). In 1984 a consortium obtained a permit for full-scale open pit mining and subsequent gold recovery by the heap-leach process (Pendleton, and others, 1995). Open pit operations began at the Summitville Complex on South Mountain in 1985; however, actual gold recovery did not begin until 1986 (Harry Posey, Colorado D.N.R., written. com., 1995). Open pit excavation continued through October 1991 and gold recovery continued until December 1992, when the consortium declared bankruptcy (Pendleton, and others, 1995).

Ground water at South Mountain occurs in shallow perched aquifers; in addition, numerous springs and seeps (including several currently sealed or partially sealed adits) occur throughout the area. All these shallow systems discharge to the local surface waters (Cropsy Creek and Wightman Fork) in response to precipitation (Pendleton, and others, 1995). Cropsy Creek flows into Wightman Fork; Wightman Fork flows into the Alamosa River some 7.2 km below its confluence with Cropsy Creek (fig. 1). Prior studies indicate that the pH of waters from the adits, seeps, springs, and streams range from 1.7 to 3.8 (Plumlee, and others, 1995).² Further, dissolved metal concentrations range from 10^5 mg l^{-1} for Fe and Al; 10^2 to 10^3 mg l^{-1} for Cu and Zn; and 10^2 g l^{-1} to 10 mg l^{-1} for As, Cd, Cr, Co, and Ni (Bove, and others, 1995; Kirkham, and others, 1995; Pendleton, and others, 1995; Plumlee, and others, 1995).



Base modified from U.S. Geological Survey
Antonito 1:100,000, 1985

Figure 1. General location map of the Summitville area including Wightman Fork, the Alamosa River, and Terrace Reservoir.

Terrace Reservoir is located about 27 km downstream from the confluence of Wightman Fork and the Alamosa River (fig. 1). The reservoir is the first impoundment on the river downstream of Wightman Fork, and was formed by a bottom-draining earthen dam emplaced in the Alamosa River canyon between 1908 and 1912. During its history, the reservoir was completely drained in 1970 and 1982; further, it was heavily drawn down between 1956 to 1959 to

effect repairs to the dam. The reservoir trends northwest, is about 3 km long, and varies in width from 45 m to nearly 500 m. Water depths vary, but can exceed 35 m in the old river channel near the southeastern end of the reservoir near the dam (fig. 1). Maximum depths occur toward the end of spring snowmelt, and prior to the start of the spring/summer release period. Reservoir water is used in the San Luis Valley primarily for crop irrigation and to water domestic livestock (Erdman, and others, 1995).

Few data are available concerning trace element cycling into and out of Terrace Reservoir. As the first impoundment on the Alamosa River below the confluence of Wightman Fork, the reservoir represents the most likely site for metal storage from the trace element-rich acid mine drainage derived from South Mountain. Further, if the reservoir does function as a trace element sink, it also could represent a potential source for the redistribution of a variety of these elements throughout the San Luis Valley.

PURPOSE

In 1994, the U.S. Environmental Protection Agency requested that the U.S. Geological Survey (USGS) conduct an extensive bed sediment geochemical survey in Terrace Reservoir. There were three objectives of the survey: (1) to determine the trace element concentrations and their geochemical partitioning in surface and near-bottom bed sediments, (2) to determine a geochemical history of the lake using various radiometric dating techniques, and (3) to determine if recent heap-leach mining operations had a detectable impact on the reservoir. This report presents the results of this survey.

METHODS OF INVESTIGATION

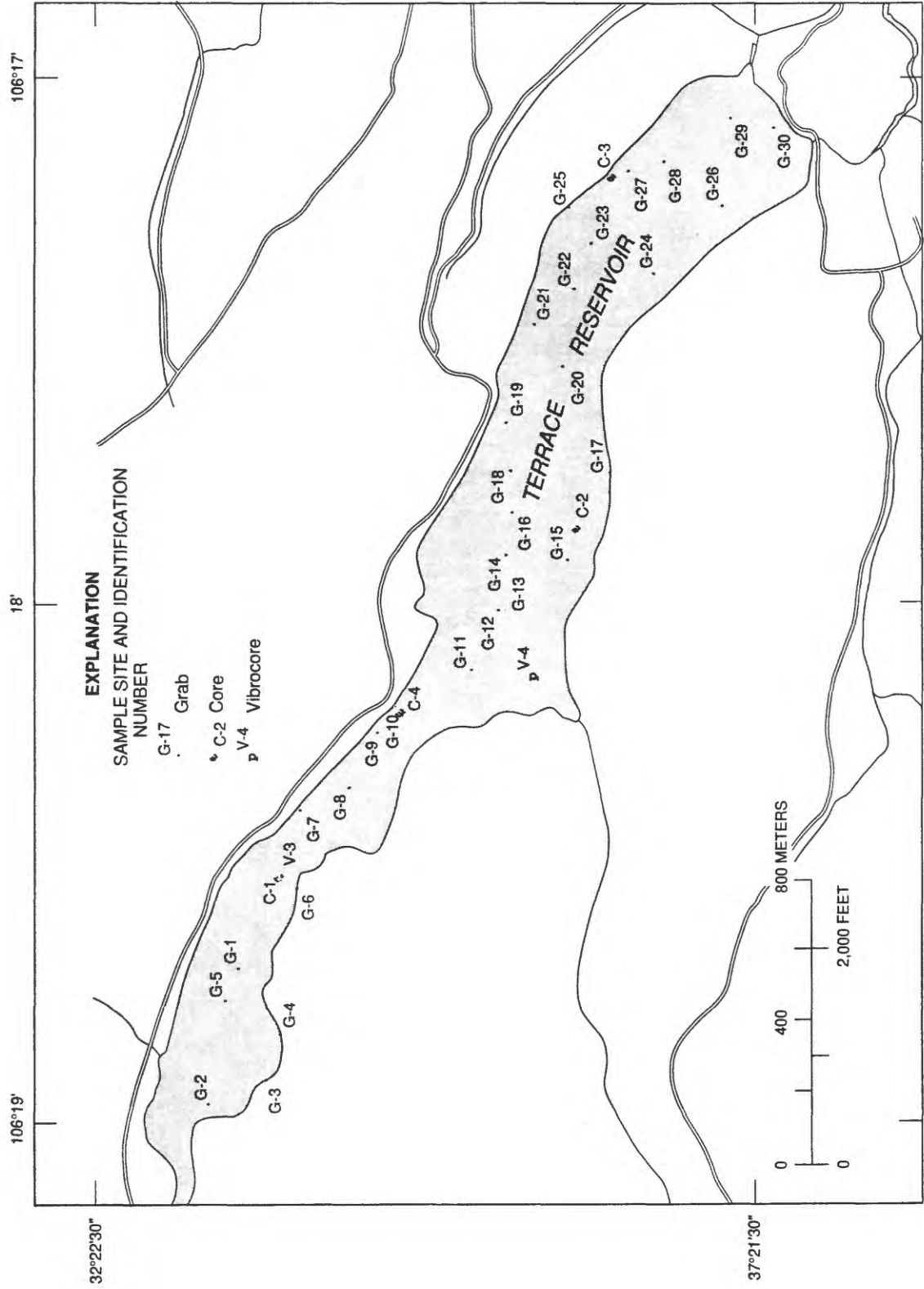
During July and August 1994 surface and near-surface bed sediments were collected in Terrace Reservoir. Surface sampling sites were randomly selected from a 5 second (150 m) square grid system; 30 surface sediment samples (fig. 2) were collected using a stainless steel Ekman grab. Although the grab collected material from depths up to 20 cm, the actual samples were limited to the upper 2 to 3 cm. These subsamples were obtained by scraping polypropylene sample cups across the surficial sediment in the grab. Care was taken to collect material away from the metallic portions of the sampler. Immediately after collection, the samples were stored at 4 °C and maintained at that temperature during shipment to Atlanta, Ga. Upon arrival, the samples were refrigerated until processed.

Initial plans called for the selection of coring sites based on bed sediment textural variations observed during the initial surface survey. However, all the collected surface sediments appeared to be similar. Therefore, gravity cores were located at long-term water quality monitoring sites in the reservoir (fig. 2). Four gravity cores, ranging in length from 67 to 94 cm were obtained using a 5 cm diameter, stainless steel 2.44 m corer with a clear polycarbonate liner and a non-metallic core catcher. Upon recovery, the liner was removed from the core barrel, kept in a vertical position, and capped at both ends. Any water remaining in the liner at the sediment-water interface was removed through a small hole to prevent any additional disturbance of the surface and near-surface sediments. After draining, the liner was trimmed to remove excess material, recapped, and the caps taped in place. The cores were stored at 4 °C and maintained at that temperature during shipment to Atlanta. Upon arrival, the cores were frozen to facilitate splitting.

The length of the gravity cores was disappointing because bottom sediment thicknesses in the reservoir had been estimated to be greater than 200 cm. Therefore, additional cores were obtained using a vibrocore with a 9.1 m long, 7.5 cm diameter barrel. Based on estimates of sediment thickness, and the requirement that the drive system for the vibrocore could not be submerged, water depths were limited to less than 6.1 m. A total of four vibrocores ranging in length from 46 to 137 cm were obtained; one was collected in the Alamosa River floodplain upstream of the reservoir, one was obtained in the river, again upstream of the reservoir, and two were collected in the reservoir proper (fig. 2).

Sample Pretreatment

Each surface grab sample was homogenized using an acid-rinsed glass rod and sieved through a 2,000- μ m polyester screen to remove overly large material (wood chips, leaf litter, etc.); the samples were then freeze dried. Appropriate-sized aliquots were removed for specific procedures using an acrylic riffle splitter or by 'coning and quartering'. Where necessary, aliquots for bulk chemical analyses were ground to <100 mesh using a sealed ceramic ball mill.



Base modified from U.S. Geological Survey
Terrace Reservoir 1:24,000, 1967

Figure 2. Detailed map of Terrace Reservoir including all surface (grab) and subsurface (coring) sampling sites.

Each core was split while frozen; one half was returned to the freezer for archiving whereas the other half was thawed. Before sampling, each half-core was described and measured. Subsamples were then removed from the thawed half-core. Wherever feasible (when sufficient mass could be collected to permit subsequent analyses), individual subsamples were removed from obvious layers, or where significant color or textural changes could be visually identified. Wherever the core appeared to be homogeneous, sampling was restricted to 5 cm intervals. Aliquots were removed using a non-metallic spatula and stored in separately labeled polypropylene vials. The vials containing the samples were returned to the freezer for storage until they could be freeze-dried. In all, 138 subsamples were obtained from the eight cores.

Analytical Techniques

Chemical analyses for Fe, Mn, Al, Ti, Cu, Zn, Cd, Pb, Ni, Co, Cr, As, Sb, and Hg were made following a slight modification of the procedures of Horowitz, and others, (1989). For all chemical elements other than As, Sb, and Hg, 500 mg aliquots were digested with a combination of HF/HClO₄/*aqua regia* in Teflon[®] beakers at 200 °C; the resulting salts were dissolved using 50 ml of 2% HCl. Determination was by ICP-AES using mixed-salt standards and interelement correction factors (appendix 1). The same digestion procedure was used for As and Sb, but final solutions were made up in 50% HCl. Arsenic and Sb were determined after the addition of urea and an oxalic acid/hydroxylamine solution and subsequent reduction using KI. Determination was by hydride generation AAS (appendix 1). Mercury was determined using 500 mg aliquots digested with LeFort *aqua regia* at 100 °C and a cold vapor technique (appendix 1). Precision and bias (usually better than ±10%) were monitored by replicate analyses of selected samples and by the concomitant digestion and analysis of National Institute of Science and Technology (NIST) sediment and USGS rock and soil standards, and are similar to those reported in Horowitz and Elrick (1985), and Elrick and Horowitz (1985; 1987). Total carbon (TC) was determined by the evolution of CO₂ using a carbon analyzer (appendix 1). Precision was better than ±10%; no bias was detected.

Geochemical Partitioning

Geochemical partitioning was determined on selected samples using a combination of physical separation and partial chemical extractions. Initially, samples were subjected to a heavy-mineral flotation to separate any sulfide minerals prior to carrying out a series of partial chemical extractions. The initial flotations were performed to prevent potential interpretational ambiguities that could be associated with the organic phase extraction which could partially or totally solubilize sulfide minerals. The flotations were made using a combination of bromoform ($\rho = 2.96 \text{ g cc}^{-1}$), and 100 μl of surfactant, to prevent flocculation. A 10 g sample was floated on 50 ml of heavy liquid in a 50 ml polypropylene centrifuge tube. The tube was spun at 2,000 rpm (RCF = 400 x g) for 30 min. The heavy mineral fractions which accumulated at the bottom of the centrifuge tubes were frozen with liquid nitrogen and the supernate and light fraction decanted. The light fractions were washed three times with acetone, followed by a deionized water rinse to remove the any remaining bromoform and acetone, and oven dried at 105 °C prior to chemical analysis. The frozen heavy mineral fractions were thawed at room temperature, and treated in the same manner as the light fractions.

Operationally defined geochemical phases were determined for the light fractions using selected procedures from the methods developed by Tessier, and others, (1979) and Chao and Zhou (1983) to partition the trace elements into (1) adsorbates, (2) those associated with Mn oxides and reactive Fe, (3) those associated with Fe oxides, and (4) those associated with an organic phase (e.g., Horowitz, and others, 1995). Precision and bias for the partial chemical extractions and subsequent chemical analyses were monitored using a variety of standard reference materials and sample duplicates. Precision was better than ±10%; no bias was detected. The partitioning studies were undertaken to try to clarify ongoing geochemical processes in the reservoir, and are not necessarily a reflection of bio- and/or environmental availability.

Radiometric Dating Measurements

Two different radiometric dating techniques were used in an attempt to develop a geochemical history of the reservoir. The first method exploits ¹³⁷Cs atmospheric fallout ($t_{1/2} = 30.2\text{y}$) to water bodies from above-ground nuclear weapons testing (appendix 2). Often, a clear ¹³⁷Cs peak in a sediment core can be reliably associated with the occurrence of maximum deposition during 1963-1964; in addition, a secondary peak for 1959 can be identified. The onset of detectable ¹³⁷Cs deposition dates to 1953. This technique has been used extensively to estimate average post-1960's sediment accumulation rates in lakes and reservoirs (Ritchie and McHenry, 1984).

The second technique employs ^{210}Pb (Robbins, 1978; appendix 3). This radioisotope is a member of the following abbreviated uranium-series decay sequence: ^{238}U ($t_{1/2} = 4.5 \times 10^9 \text{ y}$) ... ^{226}Ra ($t_{1/2} = 1600\text{y}$) ... ^{222}Rn ($t_{1/2} = 4\text{d}$) ... ^{210}Pb ($t_{1/2} = 22.3\text{y}$) ... ^{210}Po ($t_{1/2} = 138\text{d}$). ^{226}Ra commonly is present in crustal materials; it decays to ^{222}Rn which leaks into the atmosphere and decays to ^{210}Pb . As a result, there is a relatively constant annual flux of this isotope to many water bodies where it accumulates in sediments. In addition to this 'excess' ^{210}Pb , normal background contributions come from the *in situ* decay of Ra in sediment matrices. In favorable cases, the decay of excess ^{210}Pb , which begins upon burial, can be used to establish sediment chronologies and information on sedimentation rates extending back about 100 y.

^{137}Cs and ^{40}K Determinations

^{137}Cs and ^{40}K (661.6 and 1460.7 KeV respectively) were determined by gamma spectroscopic analyses using a high resolution lithium-drifted planar (GeLi) detector coupled to a multichannel analyzer. The individual samples (4.00±0.01 g of dry sediment) were manually pressed to a fixed height (4.00±0.05 cm) in standardized vials to achieve conditions of constant bulk sediment density and sample shape. The system was calibrated by doping sediments of comparable composition with precisely known amounts of NIST-traceable standard solutions of radiocesium and weights of KCl. Characteristic detection limits for ^{137}Cs and ^{40}K were 0.06 and 1.0 dpm g⁻¹ respectively. This corresponds to fractional counting errors of 3% and 2% for the Cs and K over most of the range of core depths measured. ^{137}Cs was determined in both bulk samples and in separated <63-µm fractions.

^{210}Pb Determinations

Selected samples also were analyzed for ^{210}Pb and ^{226}Ra by counting gamma emissions (46.5 for the Pb and 295, 351, and 609 KeV for the Ra) from individual sample aliquots (4.00±0.01 g of dry sediment) manually pressed to a fixed height (4.00±0.05 cm) in standardized vials to achieve conditions of constant bulk sediment density and sample shape. Because the Ra determinations depended on the gammas emitted from the decay products of Rn (^{214}Pb and ^{214}Bi), the vials were sealed with epoxy cement at the sediment surface to permit in-growth and equilibration with the Rn. Samples were stored for 2 wk prior to counting in an intrinsic HpGe well detector for up to 48 h per sample. The system was calibrated by counting sediments of similar composition, density, weight, and geometry doped with precisely known amounts of NIST-traceable solutions of ^{210}Pb and ^{226}Ra . The three independent estimates of the specific activity of Ra in each sample were combined to form a single weighted average and error estimate. Characteristic detection limits for ^{210}Pb and ^{226}Ra were 0.9 and 0.1 dpm g⁻¹ respectively. These correspond to fractional counting errors ranging from 11 to 30% for ^{210}Pb and about 5% for ^{226}Ra .

Because direct gamma counting for ^{210}Pb can produce large errors, an alternative method also was used. This entailed chemical extraction prior to quantitation; as such, it generally does not recover the total activity of the radionuclide. The method is a modification of that reported by Flynn (1968) and exploits the self-plating property of ^{210}Po , the decay product of ^{210}Pb . The method requires that ^{210}Po be in secular equilibrium with ^{210}Pb . This condition usually is met within the core itself, but in addition, samples were stored dry for nearly a year prior to analysis. Concentrated HCl (20 ml) was added to 2.00±0.01 g of the <63-µm fraction of dried sediment. Precisely known amounts of NIST-traceable standard ^{209}Po solutions were added, and the mixture allowed to stand for 2 wk. The mixtures were then centrifuged; the supernate was made up to 100ml by the addition of 10% HCl, and 1.0 g $\text{NH}_2\text{OH}\cdot\text{HCl}$ was added to prevent Fe interference. After adjusting the pH to 1.8, the solutions were transferred to flasks containing mylar-backed polished Cu disks onto which the two Po isotopes (^{209}Po and ^{210}Po) self-plated over a period of 12 h. Plated disks were counted using solid-state surface barrier detectors coupled to a multichannel analyzer. The overall fractional counting error in determining extracted ^{210}Pb activities was about ±4%. A comparison of the ^{210}Pb data produced by both methods, used in conjunction with data on ^{226}Ra to estimate the concentration of supported ^{210}Pb , indicates that the HCl-extraction efficiency averaged about 50%. Further, the patterns of excess ^{210}Pb derived by using data generated by either method were comparable, within experimental error.

GEOCHEMISTRY OF BED SEDIMENTS

During sample collection, the water in the reservoir appeared relatively clear (visibility was on the order of 3 to 4 m), but had a greenish-gray cast. This color may have been due to the presence of dissolved/colloidal Cu and/or Al. During the same period, based on the surface bed sediment grab samples, the bottom of the reservoir was covered by a thin (1- to 3-cm thick), soupy, extremely fine-grained red-orange floc. Despite the closed nature of the Ekman

grab, variable amounts of the floc 'washed out' during sampling, and appeared as a fine-grained cloud trailing the sampler as it neared the surface prior to recovery. Floc losses were likely to be greatest for the deeper samples relative to the shallower ones because of increased recovery times. Based on color, it was inferred that the floc contained, or was composed of substantial quantities of Fe oxide. At least some of the chemical variability displayed by the surface grab samples (see later) could result from the amount of floc lost/retained during sampling.

The subsurface sediments were markedly more indurated than the surface sediments. Color varied with depth in the sediment column; material nearest the surface generally was light brown to tan, followed by a lighter grayish material having some thin black layers or inclusions. The majority of the sediments were fine-grained (<63- μ m), and little or no sand-sized (>63- μ m) material was present. Core lengths varied with location, but, with one exception, almost certainly do not represent actual sediment thicknesses. The exceptions are the cores obtained where the Alamosa River enters the reservoir (cores C-1 and V-3, fig. 2). Both a gravity and a vibrocore were obtained at this site and are somewhat similar in length (77 and 97 cm respectively). The vibrocore bottomed in very coarse rounded cobbles that appeared to be old river-bed alluvium. Although vibrocore V-4 was the longest core collected (138 cm, fig. 2), and is closest in length to the estimated sediment thickness in Terrace Reservoir (200 cm), it almost certainly did not bottom in river-bed alluvium. The core was stopped by a fairly fine-grained, plastic, relatively dry sediment which was highly resistant to penetration. Core C-3 came from the deepest part of the reservoir and, despite several attempts, was the shortest one collected. The cutter and catcher contained pieces (2 to 3 cm in cross-section) of what appeared to be charred wood; these probably were responsible for limiting the depth of penetration.

Bulk Sediment Chemistry

Chemical analyses of the surface grab samples from Terrace Reservoir, a mixture of indurated sediment and floc residue, indicate enrichments in Cu, Pb, Zn, Cd, As, Sb, Hg, Fe, and Al relative to unaffected fine-grained sediments collected in a variety of environments throughout the United States (Horowitz, 1991; table 1). Based on comparisons of the mean and median values, Cu concentrations are about 500 to 1000 times, and the As and Hg concentrations are about 10 times higher than typical background levels. The Zn, Pb, Cd, Sb, Fe, and Al concentrations also are elevated; however, enrichment factors only range from 1.5 to 3 times background levels. Conversely, the concentrations of Cr, Ni, Co, Ti, and Mn are within the range of normal background levels.

With the exception of the lower half of core V-4 (see below), core concentrations of Cu, Pb, Zn, Cd, As, Sb, Hg, Fe, and Al also display elevated levels relative to unaffected fine-grained sediments from around the United States (table 1, Horowitz, 1991). Based on comparisons of mean and median values, the Cu concentrations are about 35 times, and the As and Hg concentrations are about 5 to 10 times higher than background levels. These enrichments are not as great as in the surface samples. The Zn, Pb, Cd, Sb, Fe, and Al concentrations are slightly elevated, but are similar to those for the surface samples (about 1.5 to 3 times background). The differences between the surface and subsurface samples, for at least some of the elements (e.g., Cu, Zn, Fe), may reflect post-depositional remobilization, upward diffusion, and subsequent reprecipitation caused by changing physicochemical conditions (Eh, pH) in the upper sediment and lower water column (Laurie Ballistreri, USGS, oral com., 1995). Such conditions could have led to the widespread presence of the ubiquitous red-orange floc which may be authigenic, rather than detrital.

As indicated above, vibrocore V-4 was the longest core (138 cm) collected in Terrace Reservoir. The core is composed of three distinct sections. The upper section (0-51 cm) is similar in color, texture, and chemical composition to the other core and surface grab samples (appendix 1). It is 70 \pm 5% silt/clay (<63- μ m; sieve analyses) and, based on color, appears to contain Fe oxides. The middle section (51-64 cm) represents a marked textural change. Visually, it is coarser than the upper section, and there is a concomitant decrease in trace element concentrations. Grain size variability in this section is extreme; the <63- μ m percentages range from <1 to nearly 70%. The reduced chemical levels in the middle section of the core, relative to the upper section, could be ascribed to the marked increases in median grain-size (Horowitz, 1991).

The lower section of V-4 (64-138 cm) is similar in texture and color to the upper section. The <63- μ m percentage in the lower section is not quite as high as in the upper section (about 60% from 64-90 cm, about 40% from 90-138 cm). Although the upper and lower sections appear somewhat similar in color and texture, the chemical concentrations in the bottom section are markedly lower than in the upper section (table 1). In fact, the lower section chemical concentrations are at background levels (Horowitz, 1991; table 1). Although the percentage of <63- μ m material in the lower section is not as high as in the upper section, this difference is probably too small to account for the very marked chemical differences between the two. The chemical concentrations in the lower section of V-4 could represent local background chemical levels for the reservoir, as well as for the general area.

Table 1. Minimum, Maximum, Mean, and Median Element Concentrations for Bed Sediments from in and Around Terrace Reservoir

[see "Abbreviations" for definition of terms; S, concentrations from 30 surface grab samples and the top sections of 4 cores; C, concentrations from the vibro- and gravity cores collected in the reservoir; R, concentrations from 2 vibrocores collected upstream of the reservoir, one from the river and one from the floodplain; BG, concentrations from TLV-4 below the trace element-rich zone; NW, nationwide averages for fine-grained bed sediments from all over the United States (from Horowitz, 1991); ppm, parts per million;<, less than; N/A, not available; Wt. %, concentration, in percent]

Element	Number of samples	Minimum	Maximum	Mean	Median	Elements	Number of samples	Minimum	Maximum	Mean	Median
Ag ppm (S)	34	<0.5	0.9	0.4	<0.5	As ppm (S)	34	28	213	70	62
Ag ppm (C)	77	<0.5	4.4	0.8	0.6	As ppm (C)	77	14	159	45	38
Ag ppm (R)	33	<0.5	0.5	<0.5	<0.5	As ppm (R)	33	7.0	47	15	10
Ag ppm (BG)	24	<0.5	<0.5	<0.5	<0.5	As ppm (BG)	24	4.0	10	6.7	6.0
Ag ppm (NW)	N/A	N/A	N/A	N/A	N/A	As ppm (NW)	N/A	1.5	15	7.0	6.0
Cu ppm (S)	34	720	2300	1400	1500	Sb ppm (S)	34	1.1	3.1	2.1	2.0
Cu ppm (C)	77	140	2200	660	570	Sb ppm (C)	77	1.8	21	4.0	2.9
Cu ppm (R)	33	170	820	260	250	Sb ppm (R)	33	0.7	2.6	1.2	1.0
Cu ppm (BG)	24	23	70	36	30	Sb ppm (BG)	24	0.3	1.5	0.7	0.7
Cu ppm (NW)	N/A	4	43	20	17	Sb ppm (NW)	N/A	0.1	1.2	0.6	0.6
Pb ppm (S)	34	31	83	62	63	Hg ppm (S)	34	0.20	0.54	0.31	0.31
Pb ppm (C)	77	44	420	89	72	Hg ppm (C)	77	0.14	0.71	0.35	0.34
Pb ppm (R)	33	22	64	33	28	Hg ppm (R)	33	0.02	0.40	0.10	0.05
Pb ppm (BG)	24	13	30	17	16	Hg ppm (BG)	24	0.02	0.06	0.03	0.03
Pb ppm (NW)	N/A	9	47	23	22	Hg ppm (NW)	N/A	0.02	0.13	0.05	0.04
Zn ppm (S)	34	100	440	190	150	Fe Wt. % (S)	34	5.9	14.6	8.2	7.4
Zn ppm (C)	77	96	400	220	190	Fe Wt. % (C)	77	4.3	9.0	6.1	6.0
Zn ppm (R)	33	86	160	103	101	Fe Wt. % (R)	33	3.5	8.2	4.6	4.1
Zn ppm (BG)	24	83	160	106	101	Fe Wt. % (BG)	24	2.5	5.2	3.3	3.1
Zn ppm (NW)	N/A	23	200	88	85	Fe Wt. % (NW)	N/A	1.1	6.1	2.8	2.6
Cd ppm (S)	34	0.1	1.8	0.6	0.5	Mn Wt. % (S)	34	0.03	0.29	0.07	0.05
Cd ppm (C)	77	0.1	1.9	0.6	0.6	Mn Wt. % (C)	77	0.01	0.16	0.07	0.07
Cd ppm (R)	33	0.1	0.5	0.2	0.2	Mn Wt. % (R)	33	0.05	0.06	0.06	0.06
Cd ppm (BG)	24	0.1	1.2	0.5	0.4	Mn Wt. % (BG)	24	0.03	0.22	0.09	0.08
Cd ppm (NW)	N/A	N/A	N/A	N/A	N/A	Mn Wt. % (NW)	N/A	0.02	0.10	0.06	0.06
Co ppm (S)	34	9	58	22	16	Al Wt. % (S)	34	6.5	11.0	9.5	9.5
Co ppm (C)	77	9	43	21	19	Al Wt. % (C)	77	7.8	10.6	8.9	8.8
Co ppm (R)	33	11	16	13	13	Al Wt. % (R)	33	6.2	8.5	7.0	6.9
Co ppm (BG)	24	8	16	11	11	Al Wt. % (BG)	24	6.5	8.3	7.5	7.5
Co ppm (NW)	N/A	6	39	17	17	Al Wt. % (NW)	N/A	2.1	8.1	5.5	5.7
Ni ppm (S)	34	8	28	14	11	Ti Wt. % (S)	34	0.20	0.38	0.32	0.34
Ni ppm (C)	77	8	24	15	14	Ti Wt. % (C)	77	0.30	0.49	0.40	0.40
Ni ppm (R)	33	7	10	8	8	Ti Wt. % (R)	33	0.37	0.43	0.40	0.40
Ni ppm (BG)	24	10	17	12	12	Ti Wt. % (BG)	24	0.37	0.61	0.42	0.40
Ni ppm (NW)		4	66	25	23	Ti Wt. % (NW)		0.19	0.66	0.41	0.43
Cr ppm (S)	34	13	27	21	21	TC Wt. % (S)	34	1.7	4.4	2.6	2.5
Cr ppm (C)	77	17	28	19	19	TC Wt. % (C)	77	1.1	3.9	2.0	1.9
Cr ppm (R)	33	8	20	14	13	TC Wt. % (R)	33	0.1	2.4	0.5	0.2
Cr ppm (BG)	24	16	29	22	21	TC Wt. % (BG)	24	0.4	6.6	2.5	2.5
Cr ppm (NW)		20	90	51	50	TC Wt. % (NW)		0.4	5.5	1.4	1.0

The presence of background trace element levels in the reservoir was somewhat unexpected for several reasons. The Alamosa River drains several mineralized areas (Kirkham, and others, 1995); hence, some trace element enrichment would be expected from the weathering and subsequent erosion of exposed upstream ore-bearing material. Further, active surface and subsurface mining was extant in the basin for nearly 40 y (since 1875, Steven and Rette, 1960) prior to the creation of Terrace Reservoir (1908-1912), as well as during much of its existence. Mining activity almost certainly would have led to the release of trace element-rich liquids and solids. Finally, Tidball, and others, (1995) observed elevated trace element levels (especially Cu and As) associated with Alamosa River floodplain deposits downstream from the reservoir. As the chemical levels in the lower part of V-4 are on a par with those associated with unaffected fine-grained sediments collected throughout the United States, and lower (particularly for Cu, by about a factor of 2 to 3) than those associated with the Alamosa River floodplain downstream, it is possible that they do not represent background chemical levels for the Alamosa River basin, having originated from a different, more localized drainage area.

Chemical Comparisons with Sediments from the Alamosa River

The river and floodplain samples collected upstream of the reservoir, like the reservoir sediments, display elevated concentrations of Cu, As, Sb, Hg, and Fe relative to both unaffected sediments and those from the base of vibrocore V-4 (Horowitz, 1991; tables 1, 2). However, only the Cu, As, and Hg concentrations are markedly elevated over background. These elevated levels are not as high as those associated with the reservoir sediments probably as a result of two factors: (1) the river/floodplain sediments contain lower percentages of <63- μ m material, and (2) the river/floodplain sediments contain less Fe oxides (based on the total Fe concentrations in these samples) which can act as geochemical concentrators (sorption sites) for the elevated trace elements.

One Alamosa River bed sediment sample collected downstream from Terrace Reservoir indicates that there are elevated concentrations of Cu, Pb, Zn, As, Sb, and Fe relative to background (Horowitz, 1991; table 2). The downstream concentrations of Cu, Zn, Fe, and Sb are significantly higher than in the upstream sediments, whereas the concentrations of As and Hg are similar (table 2). Tidball, and others, (1995) observed a similar suite of enriched elements at similar concentrations, in surficial materials (soils, floodplain sediments, aeolian deposits) collected further downstream in the San Luis Valley. This probably indicates that Terrace Reservoir functions not only as a trace element sink, but also as a source for the downstream redistribution of several of these elements.

Chemical Comparisons of Reservoir Sediments with Sediments from Other Areas

The surface and subsurface bed sediments from Terrace Reservoir contain elevated levels of several trace elements. Of these, only Cu, As, and Hg are markedly enriched. Although Alamosa River sediments both from above and below the reservoir display elevated Cu and As concentrations, these tend to be substantially lower than those found in the reservoir itself. In comparison to river sediment samples from nearby Willow Creek, which drains heavily mineralized and mined areas, Terrace Reservoir sediments only display marked enrichments in Cu and Hg (table 2). Comparisons with bed sediments from several other Colorado rivers draining the mineralized areas around Breckenridge produce somewhat similar comparisons (table 2).

When the sediment-associated trace element concentrations from Terrace Reservoir are compared with those from other areas outside Colorado, heavily affected by either mining or other anthropogenic activities, only the Cu and As levels appear elevated (table 3). The Cu levels in Terrace Reservoir surface (maximum and median concentrations) and subsurface sediments (maximum concentration) are comparable to those in the Clark Fork River and Milltown Reservoir, both of which are downstream from the Butte-Anaconda Superfund Site, in Montana, where Cu is a major element of concern. The median Terrace Reservoir As concentrations are similar to those in affected areas in the Great Lakes, whereas the maximum concentrations are similar to those in Lake Coeur d'Alene, Idaho, which is downstream from the Bunker Hill Superfund Site (table 3).

Table 2. Comparison of Trace Element Concentrations in Terrace Reservoir Sediments with Those from Nearby Streams

[see "Abbreviations" for definition of terms; mg/kg, milligrams per kilogram; wt. %, concentration, in percent; <, less than]

Site	Ag mg/kg	Cu mg/kg	Pb mg/kg	Zn mg/kg	Cd mg/kg	Co mg/kg	Ni mg/kg	Cr mg/kg	As mg/kg	Sb mg/kg	Hg mg/kg	Fe wt. %	Mn mg/kg	Al wt. %	Ti wt. %
Terrace Reservoir - Surface															
Mean	0.4	1400	62	190	0.6	22	14	21	70	2.1	0.31	8.2	670	9.5	0.32
Median	<0.5	1500	63	150	0.5	16	11	21	62	2.0	0.31	7.4	500	9.5	0.34
Terrace Reservoir - Subsurface															
Mean	0.8	660	89	220	0.6	21	15	19	45	4.0	0.35	6.1	680	8.9	0.40
Median	0.6	570	72	190	0.6	19	14	19	38	2.9	0.34	6.0	700	8.8	0.40
Terrace Reservoir - Background.															
Mean	<0.5	36	17	106	0.5	11	12	22	6.7	0.7	0.03	3.3	860	7.5	0.42
Median	<0.5	30	16	101	0.4	11	12	21	6.0	0.7	0.03	3.1	800	7.5	0.40
Alamosa River - Upstream															
Mean	<0.5	260	33	103	0.2	13	8	14	15	1.2	0.10	4.6	560	7	0.40
Median	<0.5	250	28	101	0.2	13	8	13	10	1.0	0.05	4.1	600	6.9	0.40
Alamosa River - Downstream															
Reported value	<0.5	370	31	140	<0.1	14	8	17	13	1.6	0.07	5.8	600	7.2	0.50
Willow Creek at Creede, Co.															
Reported value	5.3	100	2000	4500	30	8	2	7	107	9.1	0.07	2.3	1900	7.9	0.27
Willow Creek near mouth, Co.															
Reported value	11.5	115	6000	7600	36	9	3	6	150	19	0.10	2.6	2100	6.5	0.25
Uncompahgre River, Co.															
Mean	2.3	470	165	910	2.3	22	14	19	34	3.9	0.08	6.2	1300	8.2	0.54
French Gulch, Co.															
Mean	3.8	130	1100	4100	12	14	34	49	52	3.6	0.27	4.2	1700	7.9	0.38
Blue River, Co.															
Mean	1.9	65	330	2000	9.3	15	32	74	20	1.8	0.24	4.2	1400	8.2	0.40
Nationwide Background															
Mean	N/A	20	23	88	N/A	17	25	51	7.0	0.6	0.05	2.8	600	5.5	0.41
Median	N/A	17	22	85	N/A	17	23	50	6.0	0.6	0.04	2.6	600	5.7	0.43

Table 3. Comparison of Trace Element Concentrations in Terrace Reservoir Sediments with Those from Other Trace Elements
 [see "Abbreviations" for definition of terms; mg/kg, milligrams per kilogram; wt. %, concentration, in percent; <, less than; N/A, not available]

Site	Ag mg/kg	Cu mg/kg	Pb mg/kg	Zn mg/kg	Cd mg/kg	As mg/kg	Sb mg/kg	Hg mg/kg	Fe wt. %	Mn mg/kg	Al wt. %	Ti wt. %
Terrace Reservoir - Surface												
Maximum	0.9	2300	83	440	1.8	213	3.1	0.54	14.6	2900	11.0	0.38
Median	<0.5	1500	63	150	0.5	62	2.0	0.31	7.4	500	9.5	0.34
Terrace Reservoir - Subsurface												
Maximum	4.4	2200	420	400	1.9	159	21	0.71	9.0	1600	10.6	0.49
Median	0.6	570	72	190	0.6	38	2.9	0.34	6.0	700	8.8	0.40
Terrace Reservoir - Background												
Maximum	<0.5	70	30	160	1.2	10	1.5	0.06	5.2	2200	8.3	0.61
Median	<0.5	30	16	101	0.4	6.0	0.7	0.03	3.1	800	7.5	0.40
Nationwide Background												
Maximum	N/A	43	47	200	N/A	7.0	1.2	0.13	6.1	1000	8.1	0.66
Median	N/A	17	22	85	N/A	6.0	0.6	0.04	2.6	600	5.7	0.43
Alamosa River - Upstream												
Maximum	0.5	820	64	160	N/A	47	2.6	0.40	8.2	560	7	0.40
Median	<0.5	250	28	101	0.2	10	1.0	0.05	4.1	600	6.9	0.40
Lake Couer d'Alene - Surface												
Maximum	21	215	7700	9100	157	660	96	4.9	16.4	24,600	9.0	0.64
Median	4.0	70	1800	3500	56	120	19	1.6	4.9	6500	8.0	0.34
Lake Couer d'Alene - Subsurface												
Maximum	83	650	27,000	14,000	137	845	215	9.9	13.7	69,000	11.0	0.65
Median	15	91	1800	2100	26	30	18	1.0	5.7	2600	8.1	0.31
Clark Fork River												
Maximum	6.1	1600	195	2100	11	N/A						

Table 3. Comparison of Trace Element Concentrations in Terrace Reservoir Sediments with Those from Other Trace Elements—Continued
 [see "Abbreviations" for definition of terms; mg/kg, milligrams per kilogram; wt. %, concentration, in percent; <, less than; N/A, not available]

Site	Ag mg/kg	Cu mg/kg	Pb mg/kg	Zn mg/kg	Cd mg/kg	As mg/kg	Sb mg/kg	Hg mg/kg	Fe wt. %	Mn mg/kg	Al wt. %	Ti wt. %
Milltown Reservoir, Montana												
Reported value	N/A	450	70	1800	6.3	N/A						
Dutch Rhine												
Maximum		470	850	3900	N/A	N/A	N/A	18	N/A	N/A	N/A	N/A
German Rhine												
Maximum		290	370	1250	13	N/A	N/A	9	N/A	N/A	N/A	N/A
Meuse River												
Maximum		290	760	2700	33	N/A						
Rotterdam Harbor												
Maximum		740	1350	3100	66	N/A						
Great Lakes												
Maximum		300	1600	2000	22	42	N/A	9.5	N/A	N/A	N/A	N/A
Los Angeles Sewer Outfall												
Reported value	8.8	300	135	N/A	21	N/A	N/A	1.7	N/A	N/A	N/A	N/A
Rio Tinto Estuary												
Reported value		1400	1600	3100	4	N/A						
Acushnet Estuary												
Reported value	40	7500	560	2300	76	N/A	N/A	3.8	N/A	N/A	N/A	N/A
Bridgeport Harbor												
Reported value		1450	525	1500	53	5.0	N/A	0.6	N/A	N/A	N/A	N/A

Trace Element Interrelations

To help infer trace element interrelations, correlation coefficients were calculated for all the bed sediment samples collected from in and around Terrace Reservoir after the data had been normalized to Ti/TC and log-transformed (table 4; fig. 3). This mathematical pretreatment has been used previously in other lacustrine environments, to clarify geochemical patterns by eliminating problems associated with 1) rapid/erratic sedimentation (normalization to the conservative element Ti) and 2) dilution from coarse-grained organic matter (normalization to total or organic carbon; Horowitz, and others, 1988; Horowitz, and others, 1993; Horowitz, and others 1995). Almost all the correlations for the entire data set appear extraordinarily high for all the elements, especially considering the number of samples involved ($n = 168$, table 4a). This is somewhat misleading, because it is more a function of the concentration ranges of the various subgroups which constitute the data set (surface, subsurface, river, and background sediments), rather than being indicative of potential cause-and-effect relations. This pattern results because of the elevated trace element concentrations associated with the surface and subsurface samples on the one hand, relative to the less elevated river and background concentrations on the other, which leads to two large groups of data points (e.g., the Cu/Pb or Cu/Sb graphs in figure 3).

As a result of the concentration range effect, more useful information about element interrelations can be obtained by looking at correlations for the various subgroups, rather than for the data set as a whole (tables 4b-4e; fig. 3). The correlations indicate that there are substantial differences between subgroups, and that there are many more significant interrelations for the river and background sediments than for the surface and subsurface reservoir sediments. Further, even where significant correlations exist for all the subgroups, the nature of the interrelations appear to be different (note that the slopes for the 'best-fit' regression lines vary between subgroups; fig. 3). All the markedly elevated trace elements (Cu, As, Hg) associated with the surface and subsurface sediments, correlate with each other, and with Fe and Al (tables 4b and 4c). This may indicate either a common source (e.g., ore minerals from Summitville/South Mountain) or a common concentrating mechanism (e.g., association with Fe oxyhydroxides or clay minerals).

The trace element interrelations for the background and river sediment subgroups are similar to each other, but substantially different from the reservoir sediments. This occurs even though the river sediments contain markedly higher concentrations for a number of trace elements (tables 4d and 4e). As with the enriched reservoir sediments, this may indicate a similar source and/or a similar concentrating mechanism. Based on visual observation (substantial amounts of a ubiquitous, but relatively thin, red veneer on the rocks, on the river floodplains, and on the bed sediments of the Alamosa River) the concentrating mechanism is likely to be the common thread for both subgroups. Based on color, this appears to be an association with Fe oxides. This does not preclude the possibility of an association with Al hydroxides as well (note the strong correlations between Fe and Al and between the various trace elements and Al); however, the red color may mask the presence of the lighter-colored Al compounds.

Geochemical Partitioning

The masses of the heavy mineral fractions separated prior to carrying out the partial chemical extractions were too small to permit subsequent chemical analysis. In all cases, the heavy mineral fractions represented less than 1% of the mass of the samples. Therefore, heavy mineral contributions to the bulk sample chemical concentrations were calculated by subtracting the chemical concentrations associated with the light fractions from those associated with the bulk samples (table 5). The lack of substantial quantities of heavy minerals, coupled with their very limited contribution to overall sediment trace element concentrations in the reservoir sediments, indicates that the ore minerals typical of the Summitville/South Mountain area, such as covellite (CuS), enargite (Cu_3AsS_4), tennantite ($\text{Cu}_{12}\text{As}_4\text{S}_{13}$), chalcopyrite (CuFeS_2), and arsenopyrite (FeAsS) probably do not directly contribute significant quantities of trace elements to the reservoir sediments.

The partial chemical extractions carried out on the light fractions from selected surface and subsurface samples, subsequent to the heavy mineral separations, indicate that with the exception of Cu, Zn, Ni, and Co, the majority of the trace elements in the reservoir sediments are associated with operationally defined residual phases (table 5; fig. 4). This group includes the enriched elements As, Pb, Cd, Sb, Fe, and Al. As such, these elements are not likely to be environmentally available, nor readily remobilizable under changing physicochemical conditions.

Table 4. Correlation Coefficients for Terrace Reservoir and Related Sediments after Normalization to Ti/TC and Log-Transformation

[only correlations >0.70 and significant at the 99% confidence limit are listed; see "Abbreviations" for definition of terms]

	Cu	Pb	Zn	Cd	Co	Cr	Ni	As	Sb	Hg	Fe	Mn	Al
Table 4a. All Terrace Reservoir Sediments, n = 168													
Cu	1.00												
Pb	0.87	1.00											
Zn	0.82	0.94	1.00										
Cd	0.71	0.88	0.95	1.00									
Co	0.81	0.92	0.99	0.94	1.00								
Cr	0.77	0.89	0.94	0.91	0.93	1.00							
Ni	0.76	0.91	0.99	0.95	0.98	0.97	1.00						
As	0.94	0.96	0.89	0.81	0.88	0.89	0.86	1.00					
Sb	0.84	0.99	0.93	0.86	0.90	0.88	0.90	0.94	1.00				
Hg	0.91	0.98	0.92	0.84	0.90	0.87	0.88	0.96	0.97	1.00			
Fe	0.89	0.93	0.95	0.89	0.94	0.97	0.95	0.95	0.91	0.93	1.00		
Mn		0.85	0.93	0.92	0.94	0.94	0.96	0.81	0.85	0.81	0.90	1.00	
Al	0.82	0.92	0.96	0.92	0.95	0.99	0.98	0.92	0.90	0.90	0.98	0.94	1.00

	Cu	Pb	Zn	Cd	Co	Cr	Ni	As	Sb	Hg	Fe	Mn	Al
Table 4b. All Terrace Reservoir Surface Sediments, n = 34													
Cu	1.00												
Pb	0.73	1.00											
Zn			1.00										
Cd			0.76	1.00									
Co			0.82		1.00								
Cr	0.89	0.83				1.00							
Ni			0.90	0.72	0.84		1.00						
As	0.85	0.70				0.85		1.00					
Sb	0.70	0.91				0.82		0.75	1.00				
Hg	0.79	0.90				0.82		0.72	0.91	1.00			
Fe	0.86	0.83				0.94	0.59	0.70	0.78	0.83	1.00		
Mn			0.75		0.89		0.77					1.00	
Al	0.89	0.85				0.97	0.57	0.81	0.84	0.86	0.97		1.00

	Cu	Pb	Zn	Cd	Co	Cr	Ni	As	Sb	Hg	Fe	Mn	Al
Table 4c. All Terrace Reservoir Subsurface Sediments, n = 77													
Cu	1.00												
Pb		1.00											
Zn			1.00										
Cd			0.80	1.00									
Co			0.96	0.75	1.00								
Cr	0.88		0.66			1.00							
Ni			0.97	0.75	0.97	0.72	1.00						
As	0.74					0.79		1.00					
Sb		0.93							1.00				
Hg						0.72		0.81		1.00			
Fe	0.92		0.70			0.97	0.74	0.76		0.74	1.00		
Mn												1.00	
Al	0.91		0.75		0.73	0.98	0.80	0.75		0.73	0.98		1.00

Table 4. Correlation Coefficients for Terrace Reservoir and Related Sediments after Normalization to Ti/TC and Log-Transformation —Continued

[only correlations >0.70 and significant at the 99% confidence limit are listed; see "Abbreviations" for definition of terms]

	Cu	Pb	Zn	Cd	Co	Cr	Ni	As	Sb	Hg	Fe	Mn	Al
Table 4d. All Terrace Reservoir Background Sediments, n = 24													
	Cu	Pb	Zn	Cd	Co	Cr	Ni	As	Sb	Hg	Fe	Mn	Al
Cu	1.00												
Pb	0.98	1.00											
Zn	0.97	0.97	1.00										
Cd	0.87	0.90	0.91	1.00									
Co	0.93	0.94	0.97	0.90	1.00								
Cr	0.94	0.95	0.99	0.90	0.94	1.00							
Ni	0.96	0.96	0.99	0.91	0.98	0.98	1.00						
As	0.92	0.92	0.94	0.94	0.93	0.93	0.93	1.00					
Sb	0.97	0.95	0.95	0.86	0.91	0.93	0.94	0.91	1.00				
Hg	0.93	0.91	0.92	0.83	0.89	0.91	0.92	0.89	0.93	1.00			
Fe	0.95	0.96	0.99	0.91	0.98	0.97	0.99	0.95	0.94	0.90	1.00		
Mn	0.79	0.79	0.84	0.84	0.91	0.79	0.86	0.89	0.81	0.76	0.88	1.00	
Al	0.92	0.95	0.98	0.92	0.96	0.97	0.98	0.93	0.92	0.89	0.99	0.85	1.00

Table 4e. All Alamosa River Sediments, n = 33

	Cu	Pb	Zn	Cd	Co	Cr	Ni	As	Sb	Hg	Fe	Mn	Al
Cu	1.00												
Pb	0.98	1.00											
Zn	0.99	0.99	1.00										
Cd	0.92	0.94	0.93	1.00									
Co	0.98	0.99	0.99	0.95	1.00								
Cr	0.97	0.99	0.99	0.94	0.99	1.00							
Ni	0.98	0.99	0.99	0.95	0.99	0.99	1.00						
As	0.97	0.99	0.98	0.95	0.99	0.99	0.99	1.00					
Sb	0.97	0.99	0.99	0.92	0.99	0.98	0.99	0.99	1.00				
Hg	0.96	0.99	0.98	0.93	0.98	0.98	0.98	0.99	0.99	1.00			
Fe	0.98	0.99	0.99	0.94	0.99	0.99	0.99	0.99	0.99	0.99	1.00		
Mn	0.98	0.99	0.99	0.94	0.99	0.99	0.99	0.99	0.99	0.98	0.99	1.00	
Al	0.98	0.99	0.99	0.94	0.99	0.99	0.99	0.99	0.99	0.98	0.99	0.99	1.00

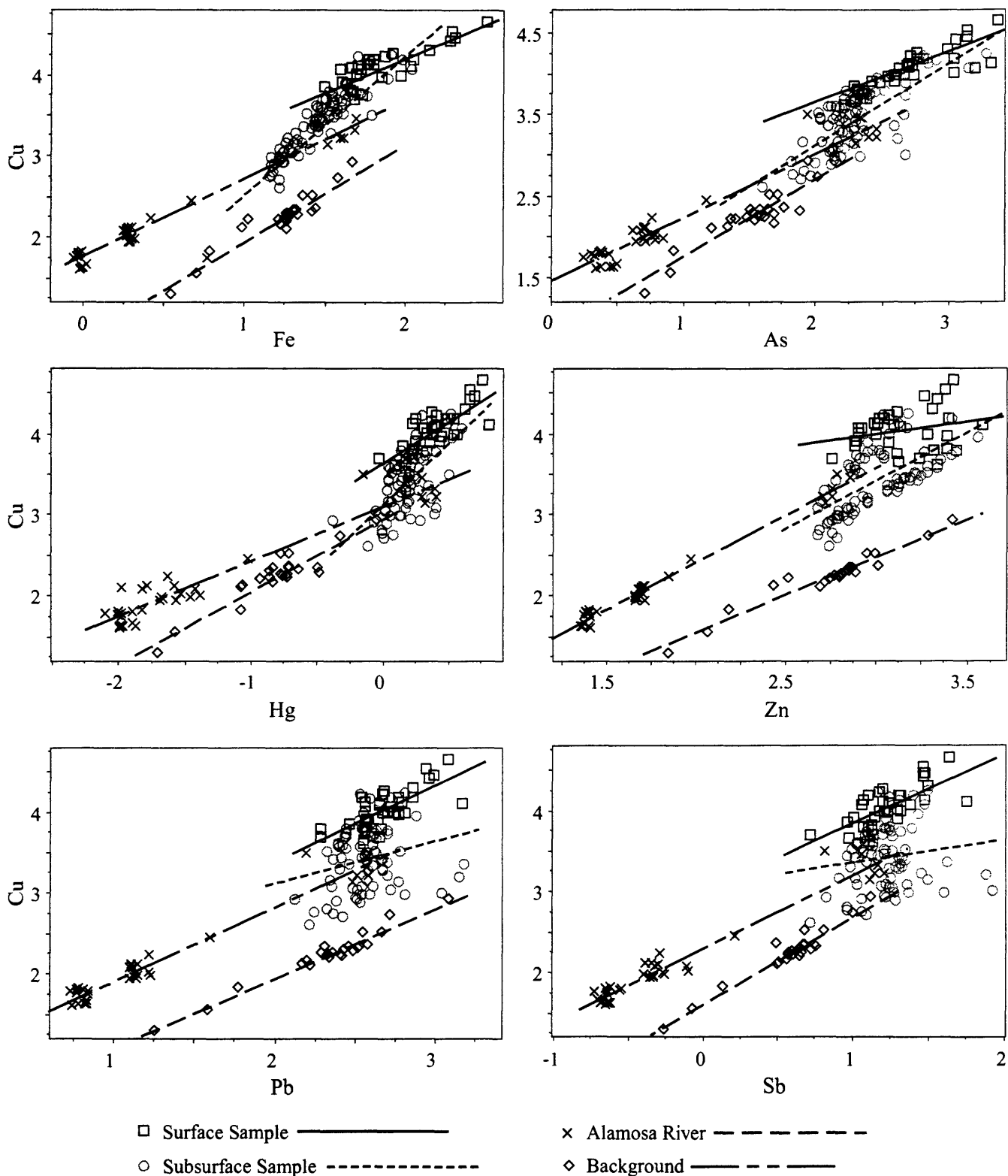


Figure 3. Selected plots of correlation coefficients comparing surface, subsurface, river, and background samples collected in and around Terrace Reservoir. The coefficients were calculated after normalization to Ti/TC and log transformation (see Horowitz and others, 1993).

Table 5. Geochemical Partitioning of Selected Sediment Samples from Terrace Reservoir

[see "Abbreviations" for definition of terms; ppm, parts per million; %, weight percent; cm, centimeters]

Sample	Extraction	Cu ppm	Pb ppm	Zn ppm	Cr ppm	Ni ppm	Co ppm	As ppm	Sb ppm	Fe %	Mn %	Al %
V-4: 0-4.5cm	Bulk	920	52	340	20	25	36	28	1.8	6.2	0.06	9.1
	Light	850	53	350	18	24	33	26	1.9	5.9	0.06	9.3
	Heavy	70	<1	<1	2	1	3	2	<0.5	0.3	<0.01	<0.1
	Adsorbates	115	<1	28	<1	1	3	<1	<0.5	0.1	0.01	<0.1
	Mn Oxide/Reactive Fe	145	<1	28	<1	1	3	<1	<0.5	0.1	<0.01	0.1
	Fe Oxide	220	<1	42	<1	3	7	<1	<0.5	1.0	<0.01	0.5
	Organic	220	<1	93	2	8	8	<1	<0.5	0.5	<0.01	0.4
	Residual	225	43	150	16	12	13	23	1.7	4.0	0.03	8.2
	Σ Cal Total	925	43	340	18	25	34	23	1.7	5.7	0.04	9.2
V-4: 25-30cm	Bulk	560	71	307	18	22	35	33	2.6	6.1	0.07	9.1
	Light	470	70	295	15	22	29	28	2.5	5.4	0.06	9.5
	Heavy	90	1	12	3	<1	6	5	0.1	0.7	0.01	<0.1
	Adsorbates	75	<1	20	<1	<1	2	<1	<0.5	<0.1	0.01	<0.1
	Mn Oxide/Reactive Fe	90	<1	19	<1	1	2	<1	<0.5	0.1	<0.01	0.1
	Fe Oxide	120	<1	31	<1	3	6	<1	<0.5	0.9	<0.01	0.4
	Organic	130	<1	72	1	7	8	<1	<0.5	0.4	<0.01	0.3
	Residual	145	62	150	15	11	14	28	2.4	4.2	0.04	8.5
	Σ Cal Total	560	62	292	16	22	32	28	2.4	5.6	0.05	9.3
V-4: 43-47cm	Bulk	240	260	170	20	14	19	110	19	5.1	0.08	8.9
	Light	210	280	150	17	13	17	110	19	4.5	0.07	9.0
	Heavy	30	<1	20	3	1	2	<1	<0.5	0.6	0.01	<0.1
	Adsorbates	17	<1	10	<1	<1	1	<1	<0.5	<0.1	0.01	<0.1
	Mn Oxide/Reactive Fe	40	<1	10	<1	1	1	<1	<0.5	0.1	0.01	<0.1
	Fe Oxide	49	<1	15	<1	1	2	<1	<0.5	0.5	0.01	0.2
	Organic	47	<1	30	1	3	3	<1	1.0	0.3	0.01	0.3
	Residual	68	280	80	15	8	9	102	17	3.4	0.04	7.9
	Σ Cal Total	221	280	145	16	13	16	102	18	4.3	0.08	8.4
V-4: 74-79cm	Bulk	47	15	160	28	17	15	8.7	0.8	3.2	0.19	7.2
	Light	38	12	155	22	13	12	9	1	2.8	0.15	7.3
	Heavy	9	3	5	6	4	3	<1	<0.5	0.4	0.04	<0.1
	Adsorbates	<1	<1	10	<1	<1	<1	<1	<0.5	<0.1	0.02	<0.1
	Mn Oxide/Reactive Fe	<1	<1	15	<1	1	4	<1	<0.5	0.1	0.10	<0.1
	Fe Oxide	3	<1	15	<1	2	2	<1	<0.5	0.1	0.02	0.3
	Organic	3	<1	25	4	2	1	<1	<0.5	0.2	<0.01	0.6
	Residual	31	13	80	18	7	4	6.8	0.7	2.0	0.02	6.1
	Σ Cal Total	37	13	145	22	12	11	6.8	0.7	2.4	0.16	7.0

Table 5. Geochemical Partitioning of Selected Sediment Samples from Terrace Reservoir—Continued
 [see "Abbreviations" for definition of terms; ppm, parts per million; %, weight percent; cm, centimeters]

Sample	Extraction	Cu ppm	Pb ppm	Zn ppm	Cr ppm	Ni ppm	Co ppm	As ppm	Sb ppm	Fe %	Mn %	Al %
V-4: 84-89cm	Bulk	26	16	90	24	11	8	4.5	0.6	2.5	0.03	6.6
	Light	24	18	80	22	10	7	4.3	0.8	2.3	0.03	7.4
	Heavy	2	<1	10	2	1	1	0.2	<0.5	0.2	<0.01	<0.1
	Adsorbates	<1	<1	<1	<1	<1	<1	<1	<0.5	<0.1	<0.01	<0.1
	Mn Oxide/Reactive Fe	<1	<1	2	<1	1	1	<1	<0.5	<0.1	0.01	<0.1
	Fe Oxide	3	<1	4	<1	1	1	<1	<0.5	<0.1	<0.01	0.1
	Organic	3	<1	13	2	3	1	<1	<0.5	0.2	<0.01	0.3
	Residual	19	15	59	20	7	4	4.4	0.7	2.1	0.02	6.6
	Σ Cal Total	25	15	78	22	12	7	4.4	0.7	2.3	0.03	7.0
G-3	Bulk	1400	64	100	23	10	12	210	3.0	6.0	0.05	8.8
	Light	1300	56	92	18	8	12	190	2.9	5.9	0.05	9.6
	Heavy	100	8	8	5	2	<1	20	0.1	0.1	<0.01	<0.1
	Adsorbates	200	<1	5	<1	<1	1	2	<0.5	0.1	0.01	0.2
	Mn Oxide/Reactive Fe	175	<1	5	<1	<1	1	<1	<0.5	0.1	<0.01	0.3
	Fe Oxide	290	<1	10	2	<1	2	50	<0.5	1.1	<0.01	0.7
	Organic	400	<1	15	2	1	2	10	<0.5	0.4	<0.01	0.4
	Residual	310	51	60	13	6	6	125	2.7	3.7	0.03	7.7
	Σ Cal Total	1375	51	95	17	7	12	185	2.7	5.4	0.04	9.2
G-4	Bulk	1400	63	100	24	10	14	190	2.8	6.4	0.05	9.7
	Light	1200	55	92	18	9	14	175	3.0	6.1	0.05	10.0
	Heavy	200	8	8	6	1	<1	15	-0	0.3	<0.01	<0.1
	Adsorbates	190	<1	5	<1	<1	2	2	<0.5	0.1	0.01	0.2
	Mn Oxide/Reactive Fe	135	<1	5	<1	<1	2	<1	<0.5	0.1	<0.01	0.3
	Fe Oxide	270	<1	10	2	<1	2	45	<0.5	1.1	<0.01	0.8
	Organic	410	<1	15	2	1	2	7	<0.5	0.4	<0.01	0.4
	Residual	310	51	60	14	7	6	120	2.5	3.9	0.03	7.9
	Σ Cal Total	1315	51	95	18	8	14	172	2.5	5.6	0.04	9.7
G-13	Bulk	880	69	260	18	15	25	40	1.8	7.0	0.07	10.0
	Light	670	62	240	17	15	23	35	2.0	6.6	0.07	9.8
	Heavy	210	7	20	1	0	2	5	<0.5	0.4	<0.01	0.2
	Adsorbates	90	<1	15	<1	<1	1	<1	<0.5	<0.1	0.01	<0.1
	Mn Oxide/Reactive Fe	95	<1	15	<1	<1	1	<1	<0.5	0.1	0.01	0.1
	Fe Oxide	140	<1	20	<1	1	3	<1	<0.5	0.9	<0.01	0.5
	Organic	170	<1	40	1	4	4	<1	<0.5	0.4	<0.01	0.3
	Residual	240	58	150	15	10	13	35	1.9	4.9	0.04	8.6
	Σ Cal Total	735	58	240	16	15	22	35	1.9	6.3	0.06	9.5

Table 5. Geochemical Partitioning of Selected Sediment Samples from Terrace Reservoir—Continued

[see "Abbreviations" for definition of terms; ppm, parts per million; %, weight percent; cm, centimeters]

Sample	Extraction	Cu ppm	Pb ppm	Zn ppm	Cr ppm	Ni ppm	Co ppm	As ppm	Sb ppm	Fe %	Mn %	Al %
G-13 Dup	Bulk	880	69	260	18	15	25	40	1.8	7.0	0.07	10.0
	Light	650	67	240	20	17	24	35	2.0	6.7	0.07	10.1
	Heavy	230	2	20	<1	<1	1	5	<0.5	0.3	<0.01	<0.1
	Adsorbates	90	<1	15	<1	<1	1	<1	<0.5	<0.1	0.01	<0.1
	Mn Oxide/Reactive Fe	95	<1	15	<1	<1	1	<1	<0.5	0.1	0.01	0.1
	Fe Oxide	140	<1	25	<1	2	4	<1	<0.5	1.0	0.01	0.5
	Organic	170	<1	40	1	4	5	<1	<0.5	0.4	<0.01	0.3
	Residual	260	60	160	16	11	13	30	2.0	5.0	0.04	8.9
	Σ Cal Total	755	60	255	17	17	24	30	2.0	6.5	0.07	9.8
G-22	Bulk	2300	58	160	23	9	12	90	1.9	12.9	0.05	9.4
	Light	2000	51	145	17	9	12	85	2.1	12.3	0.04	9.5
	Heavy	300	7	15	6	<1	<1	5	<0.5	0.6	0.01	<0.1
	Adsorbates	370	<1	15	<1	<1	1	<1	<0.5	0.2	0.01	0.1
	Mn Oxide/Reactive Fe	280	<1	10	<1	<1	1	<1	<0.5	0.3	<0.01	0.2
	Fe Oxide	450	<1	20	1	1	2	5	<0.5	3.5	<0.01	1.0
	Organic	410	<1	20	1	2	1	<1	<0.5	0.9	<0.01	0.4
	Residual	620	47	90	16	8	6	80	2.1	7.1	0.02	7.6
	Σ Cal Total	2130	47	155	18	11	11	82	2.1	12.0	0.03	9.3
G-29	Bulk	1000	68	200	22	17	48	45	2.1	9.7	0.13	9.4
	Light	900	70	220	19	17	51	40	2.3	9.9	0.15	9.7
	Heavy	100	<1	<1	3	<1	<1	5	<0.5	<0.1	<0.01	<0.1
	Adsorbates	195	<1	10	<1	1	12	<1	<0.5	0.1	0.04	0.1
	Mn Oxide/Reactive Fe	145	<1	10	<1	1	18	<1	<0.5	0.2	0.04	0.1
	Fe Oxide	235	<1	20	<1	2	8	<1	<0.5	2.8	0.03	0.7
	Organic	200	<1	30	1	4	3	<1	<0.5	0.8	<0.01	0.3
	Residual	190	65	140	15	9	8	40	2.2	5.6	0.03	8.3
	Σ Cal Total	965	65	210	16	17	49	40	2.2	9.5	0.14	9.5

Cu, the most enriched element associated with the reservoir sediments, displays a remarkably consistent partitioning pattern for all the enriched samples (table 5, fig. 4). On average, approximately 70% of the Cu is associated with operationally defined labile phases: 14% as adsorbates, 14% with Mn oxides/reactive Fe, 22% with Fe oxides, and 23% with organic matter. A significant proportion of Zn (about 40%), which is marginally enriched in the reservoir sediments, also is associated with operationally defined labile phases; on average 7% as adsorbates, 7% with Mn oxides/reactive Fe, 11% with Fe oxides, and 18% with organic matter. In substantial portions of the unenriched reservoir bed sediment, Ni and Co concentrations also are associated with operationally defined labile phases (34% and 54% respectively). As such, significant proportions of these elements may be remobilized under certain physicochemical (e.g., Eh, pH) conditions. The conclusions regarding mobility are supported by interstitial water studies which indicate that under certain physicochemical conditions in the reservoir, Cu, Zn, Ni, and Co can diffuse out of the bed sediments into the water column (Laurie Ballistrieri, USGS, oral com., 1995).

The partitioning patterns for Cu and Zn in two background samples (V-4: 74-79 cm, and 84-89 cm) are different from their enriched counterparts (table 5; fig. 4). Unlike the enriched samples, the majority of the Cu (about 80%) and Zn (about 70%) in these sediments are associated with residual rather than labile phases. This would indicate that most of the elevated Cu and Zn associated with the enriched surface and subsurface reservoir sediments are due to the presence of additional labile phases. Note that the Ni and Co concentrations and partitioning patterns are similar, regardless of sample type.

Sediment-Geochemical History of Terrace Reservoir

One of the reasons for obtaining cores in Terrace Reservoir was to try to determine a geochemical history of the impoundment. Attempts to establish accurate dates for various sedimentary horizons were based on ^{137}Cs and/or ^{210}Pb measurements. The geochronological interpretations of these measurements should be viewed with caution because both methods assume a relatively undisturbed sedimentary environment. Unfortunately, during the past 40 y the reservoir has undergone at least three major physical (and possibly concomitant chemical) disturbances. It was completely drained in 1971 and 1982 to effect repairs to the dam; further, between 1956 and 1959, the reservoir water levels were maintained at excessively low levels for similar reasons.

Dating efforts were concentrated on cores V-3, C-3, and V-4. Cores V-3 and C-3 were obtained at the northwestern (V-3 near the Alamosa River delta) and southeastern (C-3 near the dam) ends of the reservoir respectively (fig. 2). V-4 was obtained in a relatively shallow cove area, well away from the old Alamosa River channel and the main body of the reservoir (fig. 2). Despite its location, it was selected for two reasons: (1) it was the longest core collected, and (2) unlike all the others, contained sediments with background trace element concentrations. Attempts to establish a geochronology for the reservoir entailed measuring ^{137}Cs activities in all three cores, and ^{210}Pb and ^{226}Ra in one (V-4).

Initial attempts to date the three cores relied on the distribution of ^{137}Cs . The variations in ^{137}Cs activity with depth are markedly different in each core (fig. 5). The ^{137}Cs activity in V-3 is quite low, and the pattern is essentially constant throughout the length of the core. This would indicate that the core either came from an area of 1) substantial physical and/or biological activity such that once the sediments had been deposited, they were homogenized or, 2) that all the sediments present at the site were deposited quite recently (much later than the mid-1960's). The relatively low ^{137}Cs activities for this core would tend to support the view that the sediments at this site are recent. Further, river deltas in lacustrine/reservoir environments tend to be high energy zones; this could prevent the long-term deposition of sediments. Finally, cores collected in similar environments have displayed strong indications of physical disturbance (Horowitz, and others, 1995). Regardless of the cause, the homogeneous ^{137}Cs activity pattern precludes the use of this core for dating purposes.

The ^{137}Cs activity for C-3 is significantly higher than in V-3, and there is a marked, though fairly broad peak which begins at 23 cm, reaches a maximum at around 35 cm, and returns to lower activities around 42 cm (fig. 5). This is not an atypical pattern for ^{137}Cs activities; with the peak at 35 cm dated at 1963/1964. However, between 55 cm and the base of the core at 63 cm, a second peak appears to be emerging. As such, it is possible that the upper peak may not represent the 1963/1964 maximum. On the other hand, the emerging peak could represent a secondary ^{137}Cs peak normally dated around 1959; albeit, the separation between the 35 cm and the emerging peak appears to be too large for this to be likely. The ascribed date (1963/1964) for the upper peak would indicate an average sedimentation rate of some 1.2 cm y^{-1} between 1964 and 1994. However, estimates of lost reservoir capacity, based on bathymetric measurements, imply that average sedimentation rates for most of the reservoir were on the order of $6\pm 3\text{ cm y}^{-1}$ since 1981 (Ken Watts, U.S. Geological Survey, oral com., 1995). Even considering the relatively broad

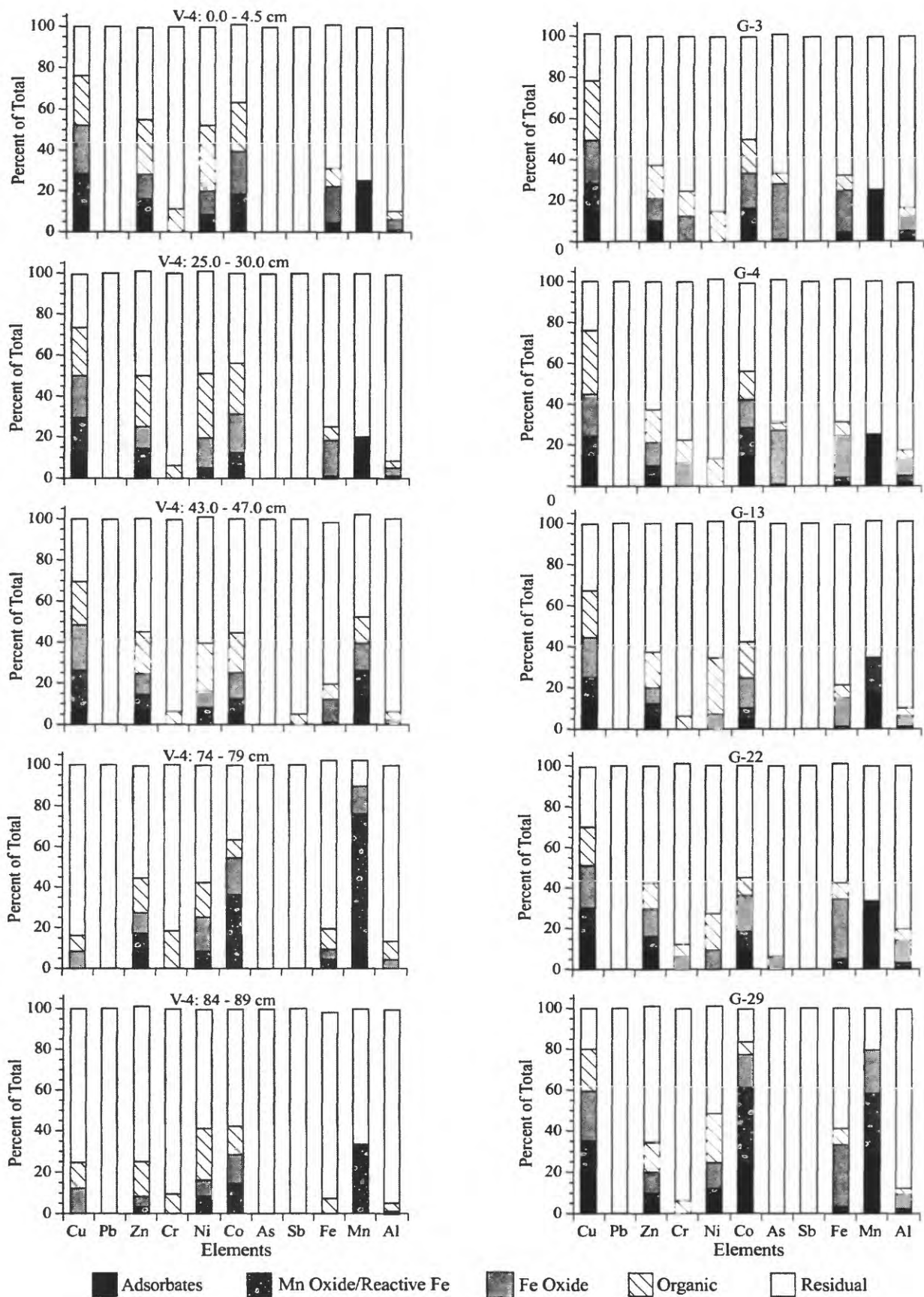


Figure 4. Graphical representation of the trace element partitioning of the light fractions of selected surface and subsurface samples from Terrace Reservoir.

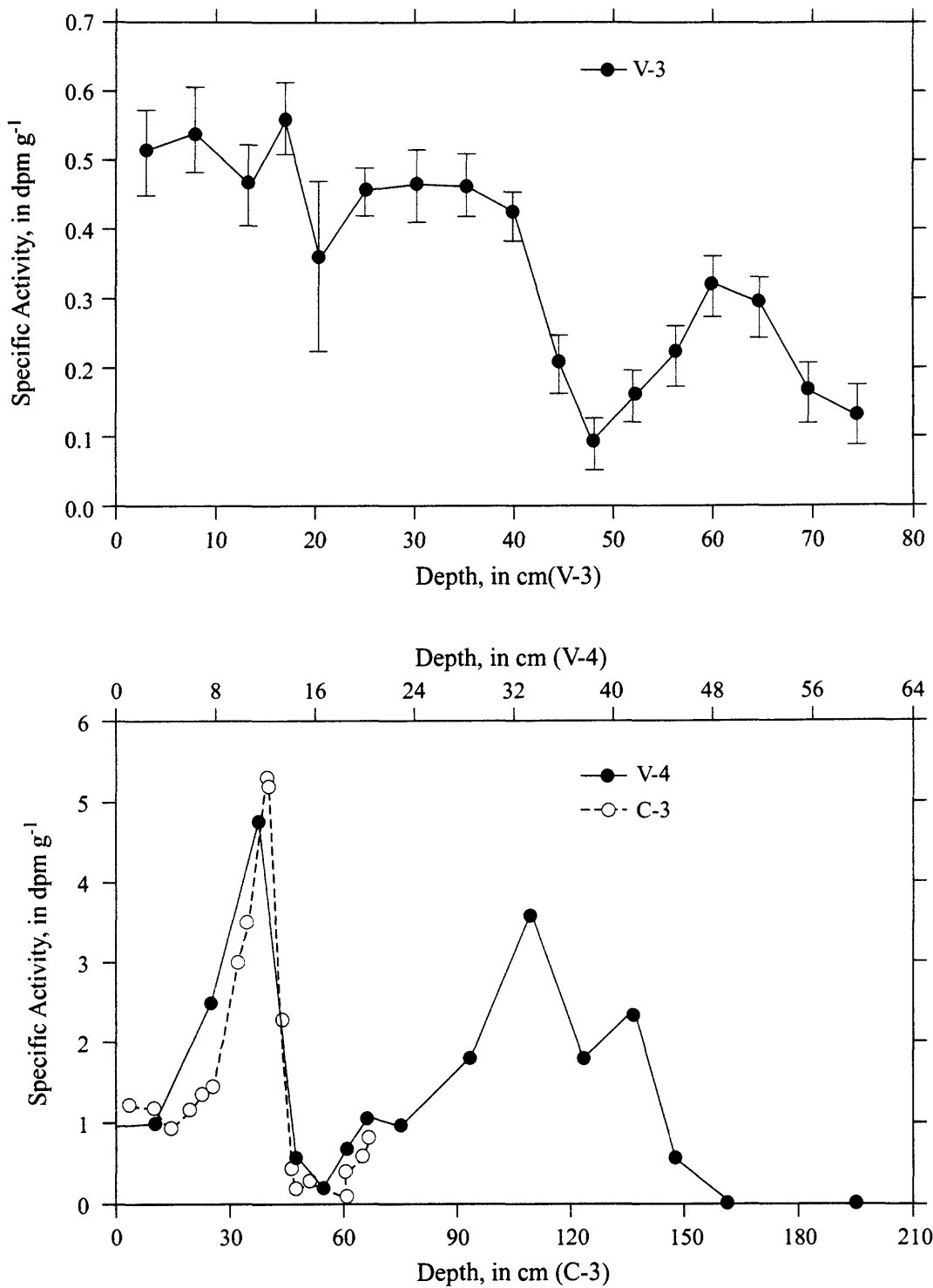


Figure 5. The distribution of ¹³⁷Cs activities with depth in three cores (V-3, C-3, and V-4) from Terrace Reservoir.

range (3 to 9 cm y⁻¹) of possible depositional rates associated with the bathymetric survey, this is markedly faster than indicated by the 1964 date for the 35-cm peak. In fact, sedimentation rates on the order of 6±3 cm y⁻¹ would date the upper ¹³⁷Cs peak at 35cm between 1983 (3cm y⁻¹) and 1990 (9cm y⁻¹). This would not be feasible if the ¹³⁷Cs associated with the 35-cm peak was derived from atmospheric fallout (see appendix 2); as such, the uppermost peak probably resulted from an internal redistribution of the particle-associated isotope from sources within the reservoir and/or the catchment (see later).

The pattern of ¹³⁷Cs activity in V-4 is atypical because it indicates the presence of two distinct and well-separated peaks of approximately equal height, at about 10 and 32 cm (fig. 5). This does not conform to the normal fallout pattern which consists of a single major peak representing the period 1963/1964. There is no measurable ¹³⁷Cs activity through or below the sharp textural boundary beginning at 51 cm. The activities in this core are similar to those found in C-3, and substantially higher than those in V-3. Examination of the V-4 ¹³⁷Cs activities associated with separated fine (<63-μm) and coarse (>63-μm) fractions from each sample aliquot indicate that the two peaks are not the result of differential dilution with ¹³⁷Cs-poor coarse material. Although unlikely, the peaks could have been caused by dilution with ¹³⁷Cs-poor fine material. Also, note the marked similarity in the ¹³⁷Cs activity patterns for both C-3 and V-4; the only difference between the two being their relative locations with depth (fig. 5).

Assuming that the sediments in V-4 have not been disturbed, the bottom of the lower peak at 45±1cm where ¹³⁷Cs is first detected should correspond to the onset of loading to the system (1953/1954). If so, then the average sedimentation rate for the entire period between 1953 and 1994 is 1.1±0.1 cm y⁻¹. Further, if the peak at 32.5±1.4cm corresponds to the 1963/1964 maximum, then the average sedimentation rate for the entire period between 1963/1964 and 1994 also would be some 1.1±0.1cm y⁻¹. If this rate is applied to an idealized ¹³⁷Cs profile (see appendix 2), and compared to actual ¹³⁷Cs measurements in V-4, there is substantial agreement (fig. 6). Note that the positions of the ¹³⁷Cs horizon (1953/1954), and the main ¹³⁷Cs peak (1963/1964) match closely. Further, the peak at 41.25±1.75 cm coincides with the secondary 1959 ¹³⁷Cs maximum in the idealized ¹³⁷Cs profile (see appendix 2), although the measured concentrations are higher than the calculated ones (fig. 6). Finally, the rate of decline in ¹³⁷Cs activity after 1963/1964 (32.5 cm) through 1980 (16 cm) is in accord with the model profile.

With the understanding that the extension of age assignments prior to the first appearance of measureable ¹³⁷Cs (1953, 45±1 cm) is a projection, a series of dates can be assigned to several stratigraphic features in V-4. The onset of trace element enrichment, which also coincides with the top of the sharp textural boundary, dates to the late 1940's. The coarse middle section between 51 and 64 cm, was deposited between the mid 1930's and the late 1940's. Finally, the change in sediment grain-size distribution (from ~60% <63-μm to ~40% <63-μm) at about 90 cm, dates to around 1912, and thus, sediments below 90 cm in the core (90 to 136 cm), would appear to have been deposited prior to the construction of Terrace Reservoir.

The onset of trace element enrichment at the top of the sharp textural boundary coincides with, and may have been caused by the cessation of active underground mining (Steven and Ratte, 1960). With the cessation of underground mining, residence times for ground water in contact with the ore body at the South Mountain/Summitville complex could increase because of reductions in physical disturbance from the mining itself, and/or because of the cessation of pumping to control subsurface water levels. In either case, this would lead to a decrease in pH, and a concomitant increase in the trace element content of the ground water. When the trace element-rich ground water contacts less acidic surface water, substantial amounts of dissolved Fe and Al will precipitate as fine-grained Fe oxides or aluminum hydroxides (depending on the final pH). In turn, these substrates can scavenge and concentrate other dissolved trace elements (e.g., Cu, Zn). Finally, these trace element-rich solid phases could accumulate in the bed sediments of Terrace Reservoir. The unconformity dates (mid-1930's to late 1940's) to a period of very high ore production at the South Mountain/Summitville complex, as measured in terms of the total annual value of gold production (Steven and Ratte, 1960). The increased gold production was almost certainly accompanied by substantial increases in the production of waste rock which, in turn, could have caused the marked changes in sediment texture associated with the unconformity or the unconformity itself.

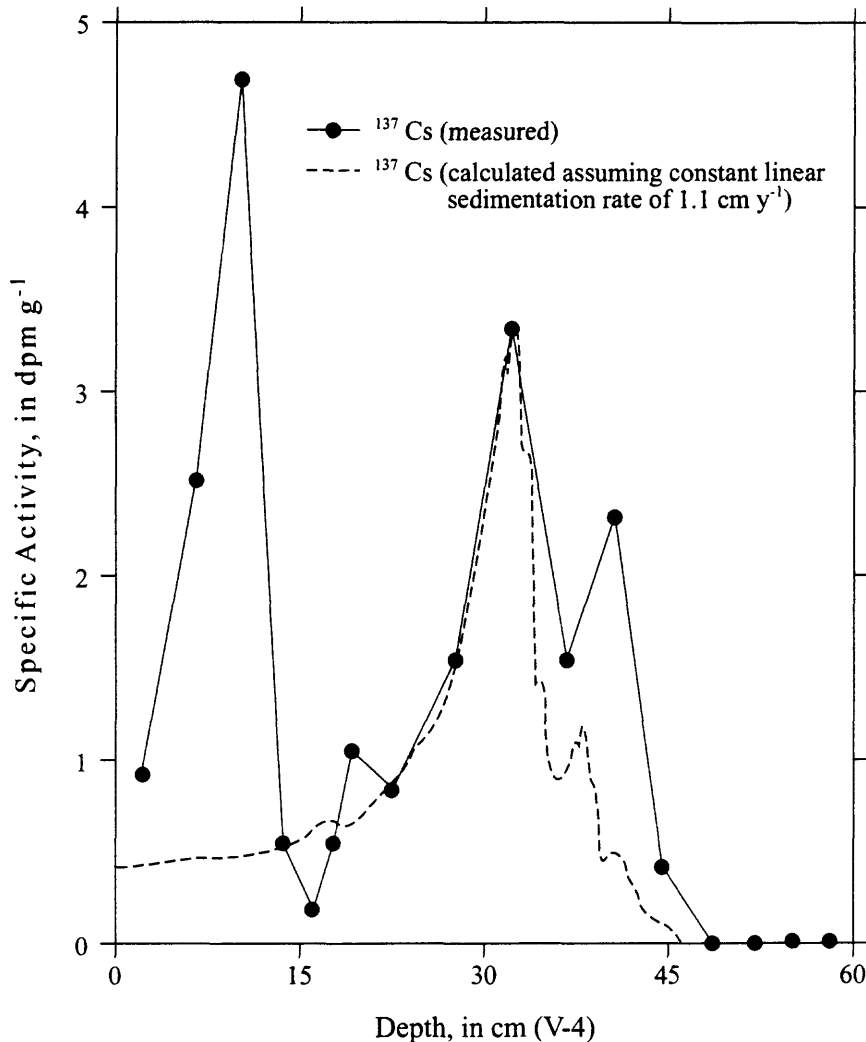


Figure 6. The distribution of ^{137}Cs with depth for core V-4 compared with a calculated distribution assuming a constant linear sedimentation rate of 1.1 cm y^{-1} .

Despite the good agreement between the idealized ^{137}Cs profile and the measured concentrations of ^{137}Cs in V-4 cited above, the idealized distribution does not account for the strong uppermost peak at $10.25 \pm 1.75 \text{ cm}$. If the mean sedimentation rate for V-4 applies to post-1980 deposition, the upper peak at $10.3 \pm 1.0 \text{ cm}$ corresponds to $1985 \pm 1 \text{ y}$. This period coincides with two occurrences which could have led to a significant internal redistribution of sediments in the reservoir and/or the catchment, and a concomitant peak in ^{137}Cs concentrations. First, annual discharge into the reservoir was markedly elevated between 1985 and 1987, relative to the 15 y period between 1980 and 1995 (Craig Cotton, Colorado Division, Engineer's Office, Alamosa, Co, written com., 1996). Annual discharge into Terrace Reservoir between 1980 and 1995 averaged $46,291 \text{ ft}^3 \text{ s}^{-1}$ (ranging from $19,548 \text{ ft}^3 \text{ s}^{-1}$ to $67,885 \text{ ft}^3 \text{ s}^{-1}$) whereas the annual discharge during the 1985/1986 period averaged $61,303 \text{ ft}^3 \text{ s}^{-1}$ ($51,258 \text{ ft}^3 \text{ s}^{-1}$ to $67,885 \text{ ft}^3 \text{ s}^{-1}$). Second, open-pit mining operations began in 1985. The combination of significantly greater discharge, along with the presence of substantial amounts of disturbed rock and soil from the 'open-pit' mining operations, could have caused the internal redistribution necessary to produce a non-atmospherically derived ^{137}Cs peak.

As noted previously, there is a marked similarity in the ^{137}Cs activity patterns for both C-3 and V-4; the only difference between the two being their relative locations with depth (fig. 5). This congruence would appear to indicate that ^{137}Cs inputs, as well as the associated sediments, were similar at both sites; although, the sedimentation rates differ by about a factor of three. If the upper (10.25 ± 1.75 cm) peak in V-4 is equivalent to the 35cm peak in C-3, and represents the same time period, then sedimentation rates at the C-3 site are markedly higher (about 3.6 as opposed to 1.1 cm y^{-1}). This is possible because the V-4 coring site is located in a relatively shallow cove area, somewhat away from the old Alamosa River channel and the main body of the reservoir (fig. 2). A sedimentation rate of 3.6 cm y^{-1} at the C-3 site is somewhat low compared to the rate derived from the 1994 bathymetric survey, but does fall within the range of error associated with that estimate ($6 \pm 3 \text{ cm y}^{-1}$). Sedimentation rate calculations based on the location of the 1963/1964 (32 cm) ^{137}Cs maximum, and the non-atmospherically derived ^{137}Cs peak dated at 1985 (10.3 cm) in V-4, would tend to support the view that post-1985/1986 deposition rates were somewhat more rapid than pre-1985/1986 rates. Post-1985 sedimentation rates at the V-4 site could have been as much as 20% higher (1.3 as opposed to 1.1 cm y^{-1}). By inference, a similar increase in sedimentation rates could have occurred at the C-3 site, based on the congruence of ^{137}Cs distributions in both cores.

In an attempt to try and confirm the ^{137}Cs geochronology, excess ^{210}Pb activities were determined for all the sample aliquots from V-4. The profile of total ^{210}Pb displays major variations over the upper half of the core (fig. 7). In contrast, ^{226}Ra activity appears relatively uniform over the length of the core, particularly above the 51 cm unconformity. Within analytical error, the activities of total ^{210}Pb and ^{226}Ra are the same below 51 cm. Extracted ^{210}Pb exhibits a similar structure as total ^{210}Pb (fig. 7). Efforts to establish an excess ^{210}Pb geochronology in V-4 were confounded by several apparent problems which make dating ambiguous, particularly: (1) a strong, almost linear correlation between excess ^{210}Pb , Cu, and several other elements, and (2) a downcore excess ^{210}Pb pattern that generally follows the normal exponential radioactive decay curve but, which displays major excursions from it (fig. 8).

Excess ^{210}Pb correlates with a number of trace elements in V-4 (Cu, Zn, Co, Fe, Al). Based on both geochemical partitioning (see the Geochemical Partitioning section of this report), as well as interstitial water studies, there are indications that several of these elements have undergone post-depositional remobilization. Therefore, the excess ^{210}Pb profile may reflect post-depositional redistribution. This could imply that the downcore excess ^{210}Pb pattern was produced by geochemical processes rather than by radioactive decay. Because any attempt to date the sediments in V-4 requires a lack of either physical or chemical disturbance, a derived ^{210}Pb geochronology could be spurious. However, it should be emphasized that correlation coefficients do not necessarily imply a cause-and-effect relation. Further, despite conditions favorable to the post-depositional remobilization of a number of trace elements in V-4, a number of previous studies have indicated that ^{210}Pb typically does not undergo such remobilization when deposition rates are as high as those indicated by ^{137}Cs (Crusius and Anderson, 1995).

As shown in appendix 3, accurate ^{210}Pb dating requires that either the accumulation rate $[R(t)]$ of excess ^{210}Pb was constant or that the rate of supply $[F(t)]$ of excess ^{210}Pb was constant (Robbins and Herche, 1993). The broad excursions displayed by the ^{210}Pb distributions in V-4, relative to a normal exponential radioactive decay curve, would imply that neither $R(t)$ nor $F(t)$ was constant, a requisite condition for excess ^{210}Pb dating. On the other hand, a plot of excess ^{210}Pb does tend to follow a calculated exponential curve based on the sedimentation rate determined from the ^{137}Cs distribution (fig. 8). As such, it would appear that the distribution of excess ^{210}Pb in V-4 adds some credence to the ^{137}Cs geochronology.

Effects of Heap-Leach Mining Activities

Based on the foregoing, it appears that the uppermost ^{137}Cs peaks in both V-4 and C-3 date around 1985/1986. This coincides with the beginning of Summitville heap-leach operations. Further, note that the onset of trace element enrichment in the reservoir bed sediments substantially predates the onset of these activities. Although the chemical variability in V-4 is substantial, the heap-leach activities do not appear to have had a detectable impact on the chemical concentrations at the V-4 site (table 6). Note the similarity in median chemical concentrations for pre- and post-heap-leach sediments (above and below the 10.25 ± 1.75 cm ^{137}Cs peak). Data for mean and maximum trace element concentrations are more ambiguous, with some being higher, and some being lower in post-heap-leach sediments. Thus, the chemical data indicate, at least at the V-4 site, that the effect of heap-leach activities on chemical concentrations probably was not major. Also note that there are some indications that the sedimentation rate at the V-4 site increased post 1985/1986. If the chemical concentrations remained about the same, while there was a potential increase in sedimentation rates, this would imply that the heap-leach operation increased the flux of trace elements to Terrace Reservoir.

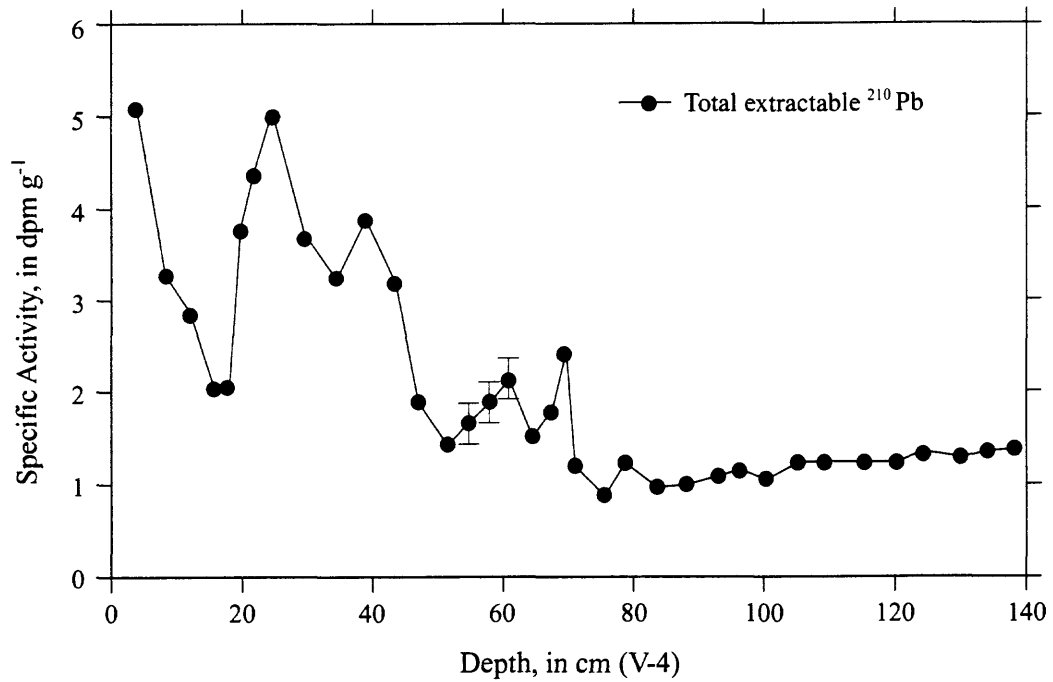
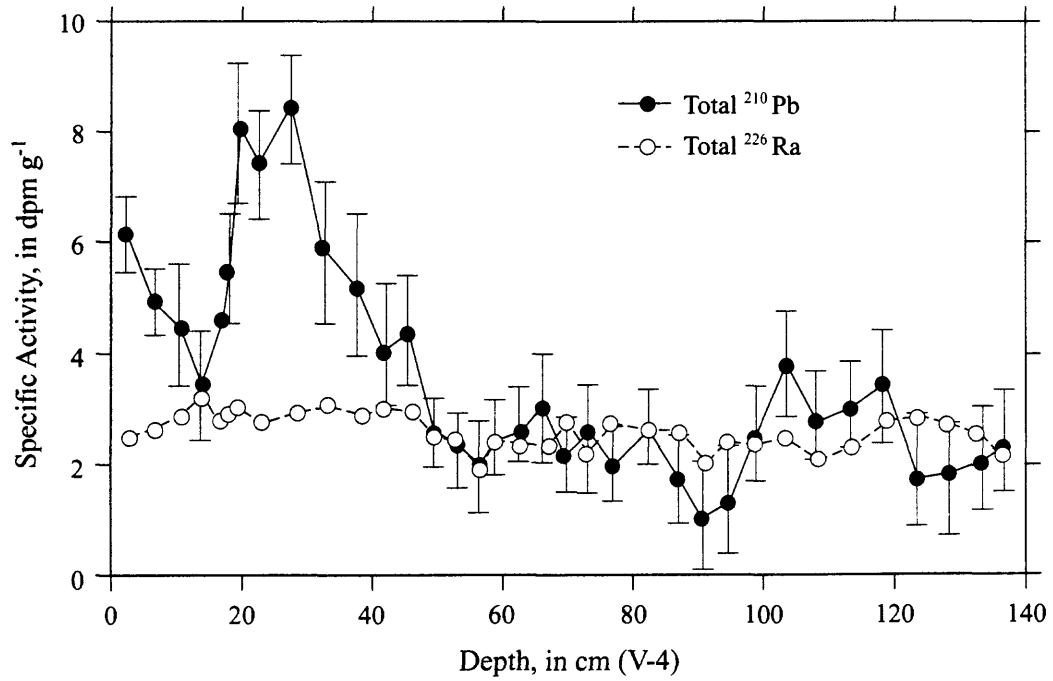


Figure 7. The distribution of total and extracted ^{210}Pb and ^{226}Ra in core V-4 from Terrace Reservoir.

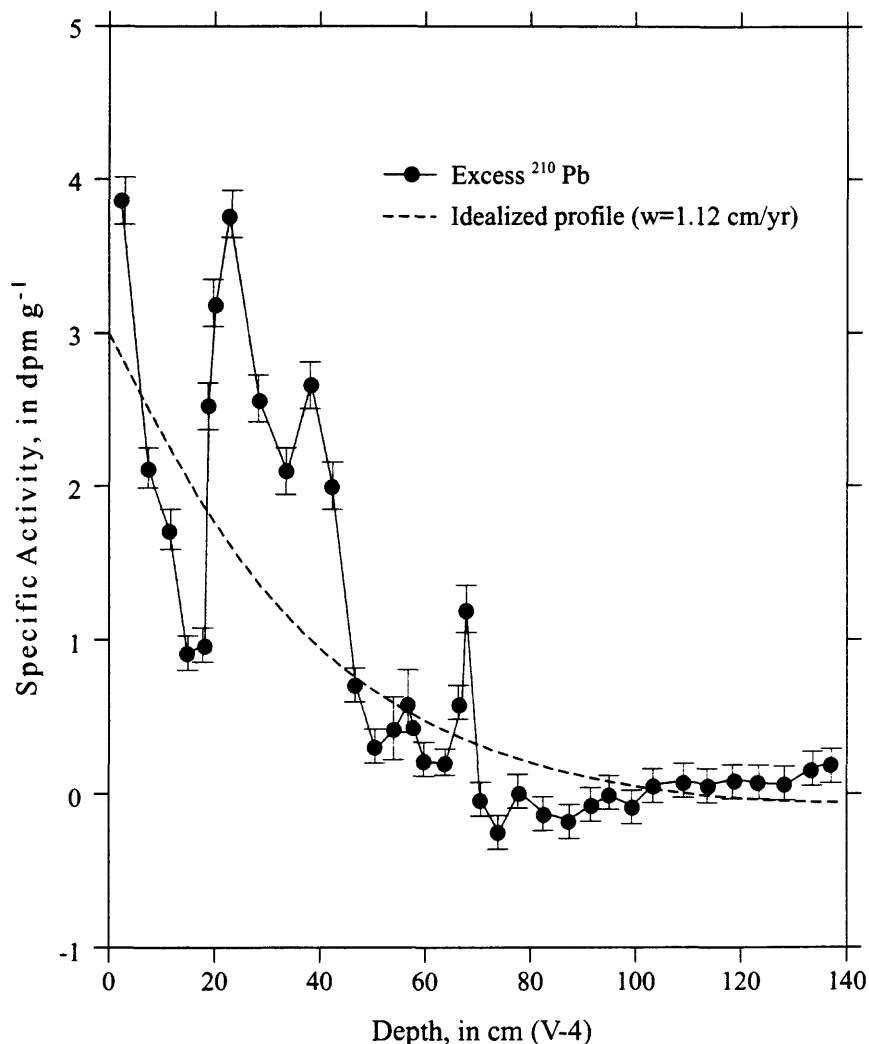


Figure 8. The distribution of excess ^{210}Pb plotted against a calculated exponential decay curve based on a linear sedimentation rate of 1.1 cm y^{-1} derived from the ^{137}Cs data from core V-4.

Based on the median trace element concentrations for pre- and post-heap-leach sediments at the C-3 site, unlike at the V-4 site, the heap-leach operation does appear to have had some chemical affect on the bed sediments. The median concentrations of Cu, Pb, Zn, Cd, and As are higher in the post-heap-leach sediments relative to the pre-heap-leach sediments (table 6). Data for mean and maximum trace element concentrations are more ambiguous, and in some cases (such as for Pb and Hg), indicate that the pre-heap-leach sediments may contain higher trace element concentrations. Based on the ^{137}Cs data from the V-4 site, and its close congruence to the ^{137}Cs data at the C-3 site, accumulation rates at the C-3 site also may have been higher during heap-leach operations. If that is the case, then even if the chemical increases at C-3 are ambiguous, there is a possibility that chemical loadings to the reservoir increased as a result of the heap-leach activities. As the C-3 site appears to be more representative of the main body of the reservoir than the V-4 site, the conclusions drawn from the C-3 data probably apply to much of Terrace Reservoir.

Table 6. Minimum, Maximum, Mean, and Median Concentrations for Core Samples Deposited Before and After the Beginning of Heap-Leach Mining Operations

[see "Abbreviations" for definitions of terms; ppm, parts per million; wt. %, concentration, in percent; <, less than]

Element	Post-Heap Leach Mining Operations				Pre-Heap Leach Mining Operations			
	Minimum	Maximum	Mean	Median	Minimum	Maximum	Mean	Median
Core V-4								
Ag (ppm)	<0.5	1.0	0.8	0.9	<0.5	3.1	1.3	0.9
Cu (ppm)	250	920	540	490	140	750	480	490
Pb (ppm)	52	117	85	85	62	280	120	87
Zn (ppm)	165	340	250	260	155	330	250	260
Cd (ppm)	0.5	1.2	0.8	0.7	0.5	1.1	0.8	0.8
Co (ppm)	16	36	26	26	18	39	28	27
Cr (ppm)	19	20	20	20	18	20	19	19
Ni (ppm)	13	25	19	19	14	24	19	18
As (ppm)	28	45	33	30	20	110	44	34
Sb (ppm)	1.8	4.0	3.1	3.4	2.0	19	5.1	3.3
Hg (ppm)	0.20	0.31	0.27	0.28	0.26	0.60	0.33	0.29
Fe (wt. %)	4.3	6.2	5.4	5.6	4.3	6.4	5.5	5.2
Mn (ppm)	500	600	580	600	600	800	660	600
Al (wt. %)	8.2	9.3	8.9	9.0	8.6	9.1	8.9	8.9
Ti (wt. %)	0.36	0.42	0.4	0.41	0.35	0.43	0.39	0.38
Core C-3								
Ag (ppm)	<0.5	1.7	1.2	1.3	<0.5	4.4	2.6	2.6
Cu (ppm)	420	980	680	680	150	470	290	270
Pb (ppm)	66	180	96	85	44	416	150	66
Zn (ppm)	210	400	330	330	190	250	220	220
Cd (ppm)	0.6	1.9	1.3	1.3	0.2	1.0	0.6	0.6
Co (ppm)	21	43	34	34	25	28	26	25
Cr (ppm)	13	20	19	20	20	24	22	21
Ni (ppm)	13	24	20	21	17	18	18	18
As (ppm)	24	57	36	31	14	118	45	24
Sb (ppm)	2.3	9.1	4.0	3.1	1.8	21	7.2	2.9
Hg (ppm)	0.29	0.47	0.36	0.36	0.14	0.71	0.39	0.36
Fe (wt. %)	5.9	8.4	6.7	6.6	5.6	6.0	5.9	5.9
Mn (ppm)	100	1100	870	1000	1000	1600	1300	1300
Al (wt. %)	6.5	10.6	9.5	9.7	8.8	10.3	9.4	9.3
Ti (wt. %)	0.21	0.42	0.35	0.37	0.38	0.46	0.43	0.43

CONCLUSIONS

(1) Both surface and sub-surface bed sediments in Terrace Reservoir are enriched in Cu, Pb, Zn, Cd, As, Sb, Hg, Fe, and Al relative to unaffected fine-grained sediments collected in a variety of environments throughout the United States; Cu, As, and Hg display the most marked enrichments.

(2) Chemical concentrations detected in the lower half of one vibrocore are equivalent to background levels found elsewhere in the United States and may represent background trace element levels for the reservoir, as well as the area as a whole.

(3) Sediment-associated Cu, Pb, Zn, As, and Sb apparently are being exported downstream from the reservoir by the Alamosa River.

(4) The majority of the enriched trace elements (Pb, Cd, As, Sb, Fe, and Al) in the bed sediments in Terrace Reservoir appear to be associated with operationally defined residual phases; as such, these elements are not likely to be environmentally available. The exceptions are Cu and Zn; substantial portions of both are associated with operationally defined labile phases such as adsorbates, Fe oxides, Mn oxides/reactive Fe, and organic phases.

(5) Attempts to develop a geochemical history of the reservoir using ^{137}Cs and ^{210}Pb indicate that the onset of trace element enrichment substantially predates the onset of heap-leach mining operations at the Summitville site on South Mountain.

(6) There are some indications, based on median and maximum concentrations, that the onset of heap-leach mining operations may have marginally increased the concentrations of some of the already enriched trace elements in the bed sediments of the reservoir.

SELECTED REFERENCES

- Bove, D.J., Barry, T., Kurtz, J., Hon, K., Wilson, A.B., van Loenen, R.E., and Kirkham, R.M., 1995, Geology of hydrothermally altered areas within the upper Alamosa River basin, Colorado, and probable effects on water quality, in Posey, H.H., Pendleton, J.A., and Van Zyl, D. eds, *Proceedings -- Summitville Forum '95*., Colorado Geological Survey Special Publication 38, Denver, CO, 35-41.
- Callendar, E. and Robbins, J.R., 1993, Transport and accumulation of radionuclides and stable elements in a Missouri River reservoir. *Water Resources Research*, 29, 1787-1804.
- Chao, T.T. and Zhou, L., 1983, Extraction techniques for selective dissolution of amorphous iron oxides from soils and sediments. *Soil Science Society of America Journal*, 47, 225-232.
- Crusius, J. and Anderson, R.F., 1995, Evaluating mobility of ^{137}Cs , $^{239} + ^{240}\text{Pu}$ and ^{210}Pb from their distributions in laminated lake sediments. *Journal of Paleolimnology*, 13, 119-141.
- Elrick, K.A. and Horowitz, A.J., 1985, Analysis of rocks and sediments for arsenic, antimony, and selenium, by wet digestion and hydride generation atomic absorption. *Varian Instruments at Work*, AA-56, 5 p.
- Elrick, K.A. and Horowitz, A.J., 1987, Analysis of rocks and sediments for mercury, by wet digestion and flameless cold vapor atomic absorption. *Varian Instruments at Work*, AA-72, 5 p.
- Erdman, J.A., Smith, K.S., Dillon, M.A., and ter Kuile, M., 1995, Impact of Alamosa River water on alfalfa, southwestern San Luis Valley, Colorado, in Posey, H.H., Pendleton, J.A., and Van Zyl, D. eds, *Proceedings-- Summitville Forum '95*: Colorado Geological Survey Special Publication 38, Denver, CO, 263-271.
- Flynn, W.W., 1968, The determination of low levels of ^{210}Po in environmental samples. *Analytica Chimica Acta*, 43, 221-227.
- Health and Safety Laboratory (HASL), 1977, Final tabulation of monthly ^{90}Sr fallout data: 1954-1976. HASL-329, Department of Energy, New York, 401 p.
- Horowitz, A.J., 1991, *A Primer on Sediment-Trace Element Chemistry*, 2nd Ed, Lewis, Chelsea MI, 136 p.
- Horowitz, A.J. and Elrick, K.A., 1985, Multielement analysis of rocks and sediments by wet digestion and atomic absorption spectroscopy. *Varian Instruments at Work*, AA-47, 7p.
- Horowitz, A.J., Elrick, K.A., and Callendar, E., 1988, The effect of mining on the sediment-trace element geochemistry of cores from the Cheyenne River arm of Lake Oahe, South Dakota, U.S.A. *Chemical Geology*, 67, 17-33.

- Horowitz, A.J., Elrick, K.A., and Cook, R.B., 1993, Effect of mining and related activities on the sediment trace element geochemistry of Lake Coeur d'Alene, Idaho, U.S.A. Part I: Surface Sediments. *Hydrological Processes*, 7, 403-423.
- Horowitz, A.J., Elrick, K.A., and Hooper, R., 1989, The prediction of aquatic sediment-associated trace element concentrations using selected geochemical factors. *Hydrological Processes*, 3, 347-364.
- Horowitz, A.J., Elrick, K.A., Robbins, J.A., and Cook, R.B., 1995, Effect of mining and related activities on the sediment trace element geochemistry of Lake Coeur d'Alene, Idaho, U.S.A. Part II: Subsurface Sediments. *Hydrological Processes*, 9, 35-54.
- Kirkham, R.M., Lovekin, J.R., and Sares, M.A., 1995, Sources of acidity and heavy metals in the Alamosa River basin outside of the Summitville mining area, Colorado, in Posey, H.H., Pendleton, J.A., and Van Zyl, D. eds. *Proceedings -- Summitville Forum '95*, Colorado Geological Survey Special Publication 38, Denver, CO, 42-57.
- Menzel, R.G., 1974, Land surface erosion and sources of ^{90}Sr in streams. *Journal of Environmental Quality*, 3, 219-233.
- Miller, K.M. and Hejt, M., 1986, A time resolution methodology for assessing the quality of lake sediment cores that are dated by ^{137}Cs . *Limnology and Oceanography*, 31, 1292-1300.
- Pendleton, J.A., Posey, H.H., and Long, M.B., 1995, Characterizing Summitville and its impacts: setting the scene, in Posey, H.H., Pendleton, J.A., and Van Zyl, D. eds, *Proceedings -- Summitville Forum '95*, Colorado Geological Survey Special Publication 38, Denver, CO, 1-12.
- Plumlee, G.G., Smith, K.S., Ficklin, W., Mosier, E.L., Montour, M., Briggs, P., and Meier, A., 1995, Geochemical processes controlling acid-drainage generation and cyanide degradation at Summitville, in Posey, H.H., Pendleton, J.A., and Van Zyl, D. eds, *Proceedings -- Summitville Forum '95*, Colorado Geological Survey Special Publication 38, Denver, CO, 23-34.
- Ritchie, J.C. and McHenry, J.R., 1984, Application of radioactive ^{137}Cs for measuring soil erosion and sediment accumulation rates and patterns: a review. *Journal of Environmental Quality*, 19, 215-233.
- Robbins, J.A., 1978, Geochemical and geophysical applications of radioactive lead isotopes. In: *The Biogeochemistry of Lead in the Environment*, Elsevier/North-Holland Biomedical Press, Amsterdam, 285-383.
- Robbins, J.A., 1982, Stratigraphic and dynamic effects of sediment reworking by Great Lakes zoobenthos. In: *Developments in Hydrobiology*, 9, Sediment/Freshwater Interaction, Proceedings of the 2nd International Symposium on Sediment-Water Interactions, Kingston, Ontario, Canada, ed. Sly, P.G., *Hydrobiologia*, 92, 611-622.
- Robbins, J.A., 1986, Great Lakes regional fallout source functions. Great Lakes Environmental Research Laboratory Technical Memorandum, ERL-GLERL-56, 21p.
- Robbins, J.A. and Herche, L.R., 1993, Models and uncertainty in ^{210}Pb dating of sediments. *Verhandlung Internat. Verein. Limnol.*, 25, 217-222.
- Santschi, P.H., Bollhalder, S., Farrenkothen, K., Lueck, A., Zingg, S., and Sturm, M., 1988, Chernobyl radionuclides in the environment: tracers for the tight coupling of atmospheric, terrestrial, and aquatic geochemical processes. *Environmental Science and Technology*, 22, 510-516.
- Scott, M.R., Potter, R.J., and Salter P.F., 1985, Transport of fallout plutonium to the ocean by the Mississippi River. *Earth and Planetary Science Letters*, 75, 321-326.
- Shukla, B.S., 1993, Watershed, River and Lake Modeling through Environmental Radioactivity. Environmental Research and Publications, Inc., Hamilton, Ontario, Canada, 227p.
- Steven, T.A. and Ratte, J.C., 1960, Geology and ore deposits of the Summitville District, San Juan Mountains, Colorado. *U.S. Geological Survey Professional Paper*, 343, U.S. Government Printing Office, Washington, D.C., 70p.
- Tessier, A., Campbell, P., and Bisson, M., 1979, Sequential extraction procedure for the speciation of particulate trace metals. *Analytical Chemistry*, 51, 844-851.
- Tidball, R.R., Stewart, K.C., Tripp, R.B., and Mosier, E.L., 1995, Geochemical mapping of surficial materials in the San Luis Valley, Colorado, in Posey, H.H., Pendleton, J.A., and Van Zyl, D. eds, *Proceedings -- Summitville Forum '95*, Colorado Geological Survey Special Publication 38, Denver, CO, 244-262.

APPENDICES

Appendix 1. Bulk Chemical Data for All the Terrace Reservoir Study Sediment Samples

[see "Abbreviations" for definitions of terms; cm, centimeters; ppm, parts per million; Wt. %, concentration. in percent; N/A, not available]

Sample	Depth (cm)	Ag ppm	Cu ppm	Pb ppm	Zn ppm	Cd ppm	Co ppm	Ni ppm	Cr ppm	As ppm	Sb ppm	Hg ppm	Fe Wt. %	Mn Wt. %	Al Wt. %	Ti Wt. %	Carb. total Wt. %	Sulf. total Wt. %
Grab	N/A	<0.5	1700	63	190	0.7	14	10	19	70	2.4	0.35	6.5	0.05	9.0	0.38	2.7	0.50
Grab	N/A	<0.5	1300	63	100	0.4	14	8	21	138	2.4	0.27	6.2	0.05	9.8	0.35	2.8	0.80
Grab	N/A	<0.5	1400	64	100	0.4	12	10	23	213	3.0	0.31	6.0	0.05	8.8	0.34	3.3	0.60
Grab	N/A	<0.5	1400	63	100	0.5	14	10	24	191	2.8	0.28	6.4	0.05	9.7	0.35	2.9	0.80
Grab	N/A	<0.5	1800	56	120	0.6	14	12	20	64	1.7	0.31	5.9	0.05	9.2	0.38	2.5	0.40
Grab	N/A	<0.5	1900	65	180	0.8	15	12	21	69	2.2	0.37	7.3	0.05	9.1	0.36	2.5	0.60
Grab	N/A	<0.5	1700	65	120	0.5	12	9	22	119	2.2	0.38	7.0	0.04	9.5	0.36	3.3	0.50
Grab	N/A	<0.5	1500	61	160	0.5	14	10	19	41	1.9	0.30	6.6	0.05	9.1	0.38	1.8	0.50
Grab	N/A	0.5	1500	67	140	0.3	16	8	20	48	1.8	0.32	7.2	0.04	9.7	0.36	2.0	0.70
Grab	N/A	0.5	1500	71	150	0.3	15	11	22	81	2.2	0.36	7.4	0.04	9.7	0.36	2.4	0.60
Grab	N/A	<0.5	1400	74	130	0.3	18	10	22	66	2.3	0.45	6.9	0.04	9.7	0.34	2.0	0.60
Grab	N/A	<0.5	2100	48	140	0.2	20	12	24	87	1.7	0.24	8.0	0.04	10.6	0.34	2.5	0.60
Grab	N/A	<0.5	880	69	260	0.5	25	15	18	39	1.8	0.29	7.0	0.07	10.0	0.37	1.9	0.40
Grab	N/A	<0.5	1100	42	125	0.2	19	16	27	47	1.1	0.20	6.9	0.05	11.0	0.37	1.7	0.60
Grab	N/A	<0.5	1900	50	140	0.3	14	9	21	68	1.6	0.23	8.7	0.04	10.3	0.33	2.4	0.70
Grab	N/A	<0.5	2100	55	120	0.3	9	12	25	105	1.9	0.26	14.6	0.03	8.7	0.20	4.4	1.00
Grab	N/A	0.9	1500	83	150	0.5	18	10	20	60	2.5	0.54	7.4	0.04	10.0	0.36	2.4	0.70
Grab	N/A	0.7	1000	31	440	1.5	48	27	17	34	2.0	0.34	7.5	0.08	10.4	0.32	2.0	0.30
Grab	N/A	0.6	1500	70	240	0.7	58	15	19	55	1.9	0.30	10.9	0.29	9.5	0.26	2.7	0.60
Grab	N/A	0.5	2100	55	150	0.3	11	9	19	67	1.8	0.27	9.6	0.04	10.3	0.30	2.6	0.70
Grab	N/A	<0.5	800	71	270	0.9	38	20	19	38	2.1	0.26	7.5	0.14	9.1	0.33	2.1	0.40
Grab	N/A	0.5	2300	58	160	0.5	12	9	23	90	1.9	0.30	12.9	0.04	9.4	0.24	3.6	0.80
Grab	N/A	0.5	1100	80	360	1.2	35	23	19	39	2.0	0.29	8.2	0.09	10.1	0.31	1.8	0.50
Grab	N/A	<0.5	730	62	370	1.0	56	28	19	28	2.2	0.21	6.1	0.10	9.0	0.38	2.2	0.20
Grab	N/A	<0.5	2000	55	135	0.5	11	11	22	61	1.7	0.29	8.6	0.04	9.9	0.29	2.5	0.70
Grab	N/A	0.6	1200	74	310	1.0	47	20	21	44	2.0	0.35	9.0	0.15	10.1	0.29	2.3	0.60
Grab	N/A	0.5	1900	64	150	0.4	13	11	24	79	2.0	0.32	13.2	0.04	9.4	0.23	3.3	0.90
Grab	N/A	0.5	1900	64	120	0.4	9	8	24	87	1.9	0.32	13.1	0.03	9.1	0.22	3.4	0.90
Grab	N/A	0.5	1000	68	200	0.5	48	17	22	47	2.1	0.36	9.7	0.13	9.4	0.28	2.7	0.70
Grab	N/A	<0.5	790	50	180	0.4	27	18	20	31	1.8	0.23	7.5	0.10	8.3	0.33	2.4	0.40
Core	0-4.9	0.5	1200	56	175	0.2	16	11	20	46	2.9	0.34	6.5	0.05	8.9	0.38	2.5	0.53
C-1	4.9-9.0	0.5	980	54	155	0.2	16	11	19	38	2.4	0.31	5.9	0.05	8.6	0.40	2.0	0.46
	9.0-13	0.5	900	54	145	0.3	16	11	19	38	2.5	0.33	5.9	0.05	8.6	0.41	1.9	0.45
	13-17	0.7	1100	67	160	0.4	19	11	21	50	2.9	0.49	6.4	0.05	8.7	0.39	2.1	0.52
	17-19.8	0.6	1700	56	160	0.2	18	11	20	85	2.4	0.39	7.0	0.05	9.2	0.36	2.9	0.56
	19.8-23.5	<0.5	1800	47	135	0.2	19	12	23	94	2.0	0.29	7.2	0.05	9.9	0.35	2.9	0.60
	23.5-25.7	<0.5	2200	44	130	0.1	18	10	19	80	1.8	0.26	6.4	0.05	9.3	0.36	2.8	0.52

Appendix 1. Bulk Chemical Data for All the Terrace Reservoir Study Sediment Samples—Continued

[see "Abbreviations" for definitions of terms; cm, centimeters; ppm, parts per million; Wt. %, concentration, in percent; N/A, not available]

Sample	Depth (cm)	Ag ppm	Cu ppm	Pb ppm	Zn ppm	Cd ppm	Co ppm	Ni ppm	Cr ppm	As ppm	Sb ppm	Hg ppm	Fe Wt. %	Mn Wt. %	Al Wt. %	Ti Wt. %	Carb. total Wt. %	Sulf. total Wt. %
	25.7-29.1	0.5	1500	56	125	0.2	16	10	23	159	2.6	0.29	6.9	0.05	9.2	0.34	3.9	0.61
	29.1-33.1	0.5	1200	51	130	0.4	15	10	20	70	2.4	0.35	6.2	0.05	8.5	0.38	2.5	0.45
	33.1-37.1	<0.5	1000	52	140	0.5	15	10	19	46	2.2	0.30	6.3	0.06	8.6	0.41	2.2	0.44
	37.1-41.3	<0.5	1300	49	155	0.4	14	10	19	49	2.2	0.25	7.0	0.05	8.6	0.36	2.6	0.48
	41.3-43	<0.5	1400	48	230	0.8	14	12	21	62	2.2	0.31	8.6	0.04	8.8	0.32	3.5	0.64
	43-47	<0.5	970	50	120	0.3	10	8	28	114	2.4	0.34	9.0	0.04	8.9	0.31	3.7	0.73
	47-51.2	<0.5	420	50	96	0.2	9	8	25	60	2.3	0.43	8.1	0.04	8.5	0.36	2.7	0.58
	51.2-56	<0.5	280	51	105	0.3	9	8	18	30	2.3	0.60	5.6	0.04	8.2	0.41	1.8	0.46
	56-57.9	<0.5	380	56	120	0.4	10	8	18	28	2.0	0.42	5.7	0.04	8.3	0.41	1.6	0.45
	57-62.9	<0.5	810	52	190	0.7	15	13	18	25	2.3	0.29	5.8	0.05	8.4	0.44	1.8	0.34
	62.9-67.9	<0.5	970	53	160	0.5	13	11	18	30	2.2	0.26	6.0	0.04	8.4	0.40	2.1	0.38
	67.9-72	<0.5	1200	51	165	0.4	13	11	18	30	2.2	0.26	6.0	0.04	8.5	0.40	2.2	0.38
	72-74	<0.5	770	50	140	0.4	12	10	17	24	2.0	0.26	5.6	0.04	8.5	0.40	2.1	0.37
	74-76.1	<0.5	800	51	150	0.3	12	10	17	25	2.1	0.23	5.7	0.04	8.3	0.41	2.0	0.35
	76.1-80.7	<0.5	730	50	135	0.4	12	10	18	29	2.0	0.23	5.8	0.04	8.3	0.41	2.1	0.35
	80.7-83.7	<0.5	940	52	150	0.3	12	10	20	48	2.5	0.25	6.6	0.04	8.6	0.39	2.6	0.43
	83.7-86.8	<0.5	680	52	135	0.3	11	10	19	37	2.4	0.24	6.1	0.04	8.4	0.41	2.2	0.39
	86.6-89.7	<0.5	590	51	125	0.2	11	10	18	32	2.2	0.25	5.9	0.04	8.5	0.42	1.9	0.37
	89.7-92.9	<0.5	470	58	110	0.1	9	9	19	33	2.1	0.25	6.3	0.04	8.9	0.41	1.8	0.47
	92.9-96.5	0.5	700	53	135	0.1	11	10	21	58	2.5	0.27	7.2	0.04	8.7	0.37	2.9	0.52
Core	0-3.1	0.7	1500	55	155	0.1	12	9	20	74	2.3	0.31	10.6	0.04	8.9	0.27	3.6	0.84
C-2	3.1-8.1	0.6	1000	65	180	0.4	16	12	20	44	2.9	0.33	7.2	0.05	8.8	0.37	2.1	0.50
	8.1-12.1	0.6	900	75	195	0.4	18	13	20	40	2.7	0.36	6.6	0.06	9.2	0.38	2.1	0.42
	12.1-15.8	0.6	970	69	280	0.7	29	17	19	34	3.7	0.33	7.6	0.08	9.7	0.35	2.2	0.41
	15.8-19	0.5	600	72	330	1.0	31	20	19	27	2.2	0.34	6.8	0.09	9.7	0.37	1.9	0.38
	19-23	<0.5	630	60	290	0.6	29	18	19	24	2.0	0.26	6.6	0.09	9.7	0.39	1.7	0.33
	23-26.6	0.6	540	67	260	0.6	28	16	18	25	2.7	0.35	5.7	0.08	8.7	0.42	2.2	0.32
	26.6-30.5	0.5	440	66	220	0.9	21	14	18	23	3.0	0.34	5.3	0.08	8.5	0.45	1.5	0.25
	30.5-33.7	0.8	630	79	300	1.0	26	18	18	33	3.2	0.36	6.2	0.08	8.9	0.41	1.5	0.30
	33.7-37.3	1.3	460	115	265	0.8	24	16	18	44	5.3	0.37	6.1	0.08	8.9	0.40	1.3	0.38
	37.3-39.4	1.4	390	114	225	0.5	21	14	17	46	5.1	0.49	5.9	0.08	8.7	0.42	1.3	0.31
	39.4-41.6	1.3	290	103	190	0.5	17	12	17	43	5.0	0.54	5.1	0.08	8.2	0.45	1.4	0.23
	41.6-44	1.1	280	104	180	0.5	16	12	17	44	5.1	0.64	5.4	0.08	8.2	0.45	1.4	0.25
	44-47.3	1.1	480	113	265	0.9	22	17	18	45	4.4	0.46	6.7	0.08	8.9	0.41	1.7	0.35
	47.3-51.7	1.0	210	88	170	0.5	17	12	19	33	4.1	0.46	5.3	0.08	8.4	0.49	1.3	0.22
	51.7-56.1	0.6	260	85	185	0.5	19	13	18	32	3.5	0.40	5.9	0.09	9.2	0.44	1.1	0.30
	56.1-57.3	1.1	410	81	265	0.6	23	18	17	33	3.5	0.34	7.0	0.07	9.0	0.40	1.9	0.35
	57.3-59.0	1.0	290	86	190	0.6	17	12	17	34	3.9	0.31	5.3	0.07	8.5	0.46	1.3	0.26
	59-63.9	1.3	310	112	190	0.6	18	13	17	43	5.7	0.37	5.4	0.07	8.4	0.45	1.4	0.29

Appendix 1. Bulk Chemical Data for All the Terrace Reservoir Study Sediment Samples—Continued

[see "Abbreviations" for definitions of terms; cm, centimeters; ppm, parts per million; Wt. %, concentration, in percent; N/A, not available]

Sample	Depth (cm)	Ag ppm	Cu ppm	Pb ppm	Zn ppm	Cd ppm	Co ppm	Ni ppm	Cr ppm	As ppm	Sb ppm	Hg ppm	Fe Wt. %	Mn Wt. %	Al Wt. %	Ti Wt. %	Carb. total Wt. %	Sulf total Wt. %
	63.9-65.8	1.3	380	110	200	0.3	20	14	18	42	5.6	0.36	5.7	0.08	8.4	0.44	1.3	0.29
	65.8-69	1.3	400	104	225	0.5	21	15	18	43	5.0	0.36	5.8	0.08	8.7	0.44	1.3	0.30
	69-73	1.4	270	118	180	0.6	17	12	17	44	6.4	0.38	5.0	0.07	7.8	0.45	1.3	0.24
	73-77.1	1.5	310	125	190	0.6	17	13	18	48	7.2	0.45	5.2	0.07	8.2	0.45	1.4	0.27
	77.1-79.4	1.5	400	134	215	0.7	19	14	18	53	7.1	0.42	5.3	0.07	8.3	0.46	1.4	0.30
	79.4-84.3	1.9	530	160	255	0.8	20	15	18	62	8.6	0.42	5.7	0.07	8.7	0.44	1.4	0.36
	84.3-87.3	2.3	360	240	230	0.7	19	16	18	77	14	0.51	5.2	0.07	8.2	0.44	1.2	0.39
Core C-3	0-5	0.7	720	82	215	1.8	21	13	13	29	3.1	0.35	5.9	0.06	6.5	0.21	3.8	0.52
	5-10	0.5	980	85	390	1.8	40	24	20	31	2.9	0.38	8.4	0.09	9.6	0.30	2.7	0.47
	10-14	<0.5	750	66	405	1.4	43	24	20	31	2.4	0.37	7.2	0.10	10.6	0.37	1.9	0.38
	14-17.3	<0.5	690	72	325	1.1	35	20	20	24	2.3	0.29	6.8	0.10	10.0	0.35	2.0	0.37
	17.3-21.1	1.3	840	75	375	1.2	40	22	20	31	3.0	0.36	6.8	0.10	10.1	0.40	2.3	0.36
	21.1-24.6	<0.5	670	85	320	1.2	34	20	18	24	2.9	0.34	6.3	0.09	9.3	0.37	1.6	0.31
	24.6-29.6	1.5	590	107	335	1.5	34	22	19	44	4.6	0.32	6.6	0.10	9.6	0.36	1.6	0.35
	29.6-33.1	1.2	580	100	350	1.9	34	21	20	36	4.2	0.35	6.4	0.11	10.0	0.37	1.7	0.36
	33.1-36.7	1.4	570	107	330	0.6	32	21	20	50	5.2	0.40	6.6	0.11	9.7	0.42	1.6	0.30
	36.7-40.3	1.7	420	179	260	0.8	25	16	19	57	9.1	0.47	6.2	0.10	9.2	0.39	1.3	0.36
	40.3-44.2	4.4	470	416	250	0.8	25	17	21	118	21	0.71	6.0	0.11	9.2	0.38	1.3	0.51
	44.2-47.3	0.8	250	73	230	0.2	28	17	21	27	3.7	0.42	6.0	0.16	10.3	0.46	1.1	0.27
	47.3-50.6	<0.5	150	59	190	1.0	25	18	20	14	1.8	0.29	5.8	0.15	9.3	0.40	1.1	0.22
	50.6-55	<0.5	70	28	135	0.3	12	13	27	9.8	1.5	0.06	4.4	0.08	7.5	0.47	1.1	0.09
	55-60	<0.5	60	30	120	0.3	15	14	26	9.5	1.4	0.04	4.4	0.08	7.1	0.46	1.0	0.11
	60-63	<0.5	280	44	220	0.5	25	18	24	21	2.1	0.14	5.6	0.10	8.8	0.46	1.4	0.18
Core C-4	0-5	0.5	1200	66	165	0.1	19	12	22	53	2.7	0.45	6.9	0.05	10.3	0.41	2.1	0.54
	5-8.1	<0.5	1400	68	165	<0.1	120	13	24	64	2.7	0.57	7.3	0.05	10.4	0.39	2.3	0.58
	8.1-10.3	1.1	1600	57	170	0.3	16	11	21	61	2.2	0.42	8.5	0.05	10.3	0.35	2.7	0.62
	10.3-15.3	0.6	660	60	145	0.3	13	10	20	37	2.0	0.30	6.6	0.05	9.7	0.41	1.8	0.50
	15.3-20.1	0.5	730	52	145	0.2	13	10	19	37	2.4	0.24	6.3	0.05	9.4	0.43	1.5	0.47
	20.1-24	0.7	1000	58	190	0.3	15	12	21	44	2.2	0.36	7.2	0.05	9.9	0.41	2.2	0.52
	24-27.3	0.5	750	75	145	0.2	12	9	24	53	2.1	0.37	7.2	0.04	11.2	0.39	1.8	0.71
	27.3-29	<0.5	670	58	135	0.3	12	9	27	72	2.0	0.32	7.7	0.04	9.7	0.36	2.3	0.65
	29-34	<0.5	170	36	135	0.1	12	9	16	21	1.8	0.05	5.2	0.05	7.9	0.48	0.2	0.23
	34-38	<0.5	270	36	200	0.5	14	11	15	13	2.0	0.08	4.8	0.05	7.7	0.46	0.4	0.23
	38.0-41.8	<0.5	160	30	110	0.1	11	9	13	11	1.4	0.07	4.4	0.05	7.8	0.42	0.2	0.21
	41.8-45.3	<0.5	400	55	135	0.3	13	10	20	29	2.0	0.31	5.6	0.05	9.2	0.42	1.8	0.35
	45.3-48.1	<0.5	450	59	150	0.4	13	10	20	29	2.1	0.38	5.9	0.06	9.6	0.44	1.8	0.38
	48.1-52	<0.5	600	55	175	0.5	14	11	20	38	2.4	0.38	6.3	0.05	8.9	0.43	1.8	0.42
	52-55.3	<0.5	590	60	165	0.4	14	11	21	40	2.6	0.42	6.6	0.05	9.1	0.44	2.0	0.44

Appendix 1. Bulk Chemical Data for All the Terrace Reservoir Study Sediment Samples—Continued

[see "Abbreviations" for definitions of terms; cm, centimeters; ppm, parts per million; Wt. %, concentration, in percent; N/A, not available]

Sample	Depth (cm)	Ag ppm	Cu ppm	Pb ppm	Zn ppm	Cd ppm	Co ppm	Ni ppm	Cr ppm	As ppm	Sb ppm	Hg ppm	Fe Wt. %	Mn Wt. %	Al Wt. %	Ti Wt. %	Carb. total Wt. %	Sulf. total Wt. %
	55.3-57.9	<0.5	550	57	170	0.4	14	11	20	34	2.5	0.55	6.3	0.05	9.2	0.45	1.8	0.42
	57.9-62.8	<0.5	470	63	155	0.3	14	11	21	37	2.7	0.62	6.2	0.05	9.4	0.44	1.7	0.41
	62.8-66.3	<0.5	480	57	170	0.4	14	11	20	31	2.5	0.66	5.9	0.05	9.3	0.46	1.7	0.39
	66.3-69.5	<0.5	560	59	170	0.4	15	12	20	36	2.8	0.60	6.1	0.05	9.1	0.44	1.8	0.40
	69.5-73	1.0	530	61	160	0.6	13	11	20	33	2.9	0.53	6.3	0.05	9.2	0.45	1.7	0.41
	73-78	0.6	350	70	135	0.4	12	10	21	38	3.0	0.98	6.3	0.05	9.7	0.45	1.6	0.44
	78-81.8	<0.5	340	67	125	0.4	11	9	21	35	1.9	0.71	6.3	0.05	10.0	0.43	1.5	0.49
Core V-1	0-4.5	<0.5	240	25	97	0.2	12	8	10	8.4	1.5	0.07	3.5	0.05	6.9	0.39	0.2	0.18
	4.5-8	<0.5	250	26	105	0.1	12	8	13	8.6	0.8	0.04	4.0	0.06	7.0	0.43	0.1	0.22
	8-10	<0.5	250	22	100	0.1	12	7	13	8.2	1.1	0.03	3.8	0.06	7.0	0.40	0.1	0.19
	10-15	<0.5	240	23	100	0.2	12	7	12	8.0	0.7	0.03	3.7	0.05	6.8	0.41	0.3	0.17
	15-18	<0.5	260	28	105	0.2	12	7	13	9.6	1.0	0.03	4.0	0.05	7.0	0.42	0.2	0.18
	18-21	<0.5	260	27	105	0.2	13	8	11	9.6	0.9	0.05	3.9	0.06	7.1	0.41	0.1	0.19
	21-24	<0.5	260	28	100	0.2	12	7	11	9.9	0.8	0.03	3.8	0.05	7.0	0.39	0.2	0.19
	24-27	<0.5	260	26	100	0.2	12	8	13	9.8	1.0	0.02	3.8	0.05	6.9	0.40	0.2	0.18
	27-32	<0.5	280	26	110	0.2	13	8	13	9.8	1.0	0.06	4.2	0.06	6.9	0.42	0.1	0.21
	32-37	<0.5	270	26	105	0.2	12	8	8	10	0.9	0.05	4.1	0.05	6.8	0.40	0.2	0.20
	37-42	<0.5	250	28	105	0.2	12	7	12	11	0.9	0.04	3.8	0.05	6.9	0.40	0.1	0.19
	42-47	<0.5	230	28	105	0.1	13	8	10	7.3	0.9	0.04	3.6	0.05	6.7	0.40	0.1	0.21
	47-49.7	<0.5	280	26	125	0.2	13	8	12	10	1.2	0.04	4.2	0.06	6.9	0.43	0.1	0.19
Core V-2	0-4	<0.5	230	36	110	0.1	13	8	14	13	1.7	0.06	4.1	0.06	7.0	0.43	0.2	0.21
	4-9	<0.5	180	29	110	0.1	14	9	13	8.9	0.9	0.04	4.1	0.06	6.9	0.41	0.2	0.20
	9-14	<0.5	180	29	110	0.1	13	9	14	9.6	1.0	0.04	4.2	0.06	6.8	0.42	0.1	0.21
	14-19	<0.5	170	23	110	0.1	13	9	15	9.2	0.9	0.04	4.0	0.06	6.9	0.41	0.1	0.19
	19.0-24.0	0.5	170	27	93	0.4	13	9	14	11	0.8	0.04	4.0	0.06	6.8	0.39	0.1	0.20
	24.0-26.0	<0.5	190	28	100	0.5	14	9	14	13	0.8	0.05	4.4	0.06	6.9	0.41	0.1	0.19
	26.0-31.0	<0.5	170	27	96	0.4	14	10	18	12	0.9	0.04	4.1	0.06	6.8	0.40	0.1	0.18
	31-36	<0.5	170	24	92	0.4	14	9	14	11	0.9	0.05	3.9	0.06	6.9	0.39	0.1	0.21
	36-38	<0.5	180	27	96	0.5	14	9	13	12	0.9	0.04	3.9	0.06	6.9	0.39	0.2	0.20
	38.0-43.0	<0.5	170	25	91	0.2	13	9	14	9.8	0.9	0.05	3.8	0.06	6.7	0.39	0.2	0.20
	43.0-48.0	<0.5	190	29	94	0.2	14	9	14	10	0.8	0.04	4.1	0.06	6.8	0.40	0.2	0.20
	48.0-50.0	<0.5	180	32	89	0.2	12	8	12	13	1.0	0.06	3.9	0.05	6.2	0.37	0.2	0.21
	50.0-56.5	0.5	210	28	96	0.3	14	9	14	12	1.1	0.08	4.2	0.06	6.8	0.41	0.2	0.19
	56.5-63.0	<0.5	290	40	96	0.2	13	7	12	15	1.6	0.09	4.7	0.06	6.7	0.40	0.4	0.24
	63.0-68.0	<0.5	280	64	86	0.2	12	8	19	47	2.6	0.40	6.7	0.05	7.7	0.38	2.3	0.42
	68.0-73.0	<0.5	250	56	98	0.3	11	8	18	36	2.3	0.36	6.1	0.05	7.7	0.40	2.2	0.43
	73.0-78.0	<0.5	280	56	98	0.3	11	8	20	42	2.3	0.32	7.1	0.05	7.7	0.39	2.3	0.47
	78.0-83.0	<0.5	330	59	90	0.3	11	8	20	44	2.2	0.36	7.6	0.05	8.2	0.37	2.4	0.52

Appendix 1. Bulk Chemical Data for All the Terrace Reservoir Study Sediment Samples—Continued

[see "Abbreviations" for definitions of terms; cm, centimeters; ppm, parts per million; Wt. %, concentration, in percent; N/A, not available]

Sample	Depth (cm)	Ag ppm	Cu ppm	Pb ppm	Zn ppm	Cd ppm	Co ppm	Ni ppm	Cr ppm	As ppm	Sb ppm	Hg ppm	Fe Wt. %	Mn Wt. %	Al Wt. %	Ti Wt. %	Carb. total Wt. %	Sulf. total Wt. %
	83.0-88.5	<0.5	460	62	115	0.4	11	9	20	35	1.8	0.30	8.2	0.05	8.5	0.37	2.3	0.57
	88.5-93.0	<0.5	820	41	155	0.4	16	10	19	22	1.6	0.17	7.3	0.06	7.6	0.38	1.5	0.42
Core V-3	0-5	1.0	1500	56	170	0.5	18	12	21	63	2.4	0.36	6.7	0.05	9.5	0.36	2.4	0.48
	5-10	0.7	1200	57	160	0.4	17	11	19	54	2.3	0.35	6.1	0.05	8.9	0.37	2.3	0.45
	10-15	0.5	1900	54	160	0.4	18	12	21	66	2.2	0.34	6.7	0.05	9.6	0.34	2.6	0.50
	15-18	<0.5	1900	53	125	0.3	16	10	19	96	2.0	0.35	6.1	0.05	9.2	0.35	3.0	0.47
	18-21.5	0.5	1700	57	115	0.3	16	9	24	224	2.8	0.36	7.1	0.05	9.6	0.32	4.6	0.67
	21.5-27	<.05	1200	57	125	0.3	14	10	20	75	2.4	0.36	6.2	0.06	8.7	0.39	2.4	0.44
	27-32	<0.5	1000	50	130	0.4	15	11	19	45	1.9	0.32	6.1	0.06	8.8	0.40	2.1	0.41
	32-37	<0.5	1400	50	135	0.3	15	11	19	58	2.0	0.32	6.7	0.06	8.9	0.38	2.5	0.44
	37-42.5	<0.5	1200	53	180	0.6	16	11	19	39	2.3	0.33	7.2	0.05	8.8	0.35	2.6	0.48
	42.5-46	<0.5	680	38	130	0.4	14	9	15	30	2.6	0.22	5.7	0.05	7.7	0.35	1.6	0.37
	46-49	<0.5	170	26	91	0.2	12	9	15	7.5	1.5	0.05	3.9	0.05	6.7	0.37	0.4	0.19
	49-54	<0.5	350	32	120	0.4	16	9	13	17	1.9	0.18	4.5	0.05	6.9	0.38	2.8	0.34
	54-58	<0.5	390	41	125	0.4	16	9	14	21	1.8	0.19	4.7	0.05	7.3	0.39	2.2	0.35
	58-62	<0.5	380	43	125	0.3	16	9	15	23	2.5	0.21	5.0	0.05	7.5	0.40	2.1	0.34
	62-67	<0.5	290	46	110	0.3	14	8	14	21	2.2	0.12	4.8	0.05	7.4	0.42	1.0	0.29
	67-72	<0.5	200	37	99	0.2	12	11	13	14	1.6	0.08	4.4	0.05	7.0	0.41	0.6	0.23
	72-76.5	<0.5	200	36	105	0.2	12	8	14	15	1.7	0.07	4.5	0.05	7.1	0.42	0.3	0.22
Core V-4	0-4.5	<0.5	920	52	340	1.2	36	25	20	28	1.8	0.24	6.2	0.06	9.1	0.36	2.6	0.24
	4.5-8.5	0.6	570	75	225	0.8	29	20	19	30	3.0	0.31	5.6	0.06	9.3	0.41	2.1	0.22
	8.5-12	1.0	410	95	220	0.5	22	17	19	45	4.0	0.31	5.5	0.05	8.9	0.40	2.0	0.21
	12-15	0.9	250	117	165	0.5	16	13	20	29	3.9	0.20	4.3	0.06	8.2	0.42	1.9	0.16
	15-17	2.1	430	280	225	0.6	20	15	19	70	7.5	0.42	5.1	0.06	8.6	0.37	2.0	0.38
	17-18.5	0.6	520	95	250	0.6	29	18	19	34	3.4	0.26	6.3	0.06	9.0	0.38	2.4	0.28
	18.5-20	<0.5	660	62	305	1.0	33	21	19	26	2.1	0.26	5.3	0.06	8.8	0.38	3.1	0.24
	20-25	<0.5	750	63	330	1.1	39	24	19	29	2.0	0.26	6.4	0.07	8.8	0.35	2.8	0.25
	25-30	0.7	560	71	305	0.9	35	22	18	33	2.6	0.27	6.1	0.07	9.1	0.37	2.2	0.24
	30-35	0.9	460	97	240	0.8	24	18	19	41	4.0	0.32	5.1	0.06	8.9	0.40	2.1	0.23
	35-39.5	0.6	600	79	300	0.9	33	22	18	32	2.9	0.30	6.1	0.06	9.0	0.37	2.0	0.26
	39.5-43	1.0	460	114	265	0.8	25	18	18	41	4.6	0.34	4.9	0.06	8.9	0.41	1.7	0.24
	43-47	3.1	240	260	170	1.0	19	14	20	110	19	0.60	5.1	0.08	8.9	0.43	1.8	0.40
	47-51	<0.5	140	72	155	0.5	18	15	19	20	3.2	0.28	4.3	0.08	8.6	0.43	1.6	0.16
	51-54	<0.5	48	22	100	0.2	16	14	19	5.5	0.9	0.06	4.2	0.11	8.3	0.49	0.7	0.04
	54-57	<0.5	30	17	110	0.1	16	13	20	3.5	0.7	0.02	4.3	0.11	8.1	0.50	2.1	0.02
	57-60.5	<0.5	30	19	100	0.2	16	14	29	7.6	0.8	0.03	5.2	0.11	8.0	0.61	0.4	0.03
	60.5-64	<0.5	27	17	83	0.2	14	10	16	5.8	0.6	0.02	3.7	0.08	7.9	0.45	0.6	0.03
	64-66.5	<0.5	51	25	130	0.7	12	12	22	6.6	0.7	0.03	3.5	0.06	7.8	0.42	2.7	0.04

Appendix 1. Bulk Chemical Data for All the Terrace Reservoir Study Sediment Samples—Continued

[see "Abbreviations" for definitions of terms; cm, centimeters; ppm, parts per million; Wt. %, concentration, in percent; N/A, not available]

Sample	Depth (cm)	Ag ppm	Cu ppm	Pb ppm	Zn ppm	Cd ppm	Co ppm	Ni ppm	Cr ppm	As ppm	Sb ppm	Hg ppm	Fe Wt. %	Mn Wt. %	Al Wt. %	Ti Wt. %	Carb. total Wt. %	Sulf. total Wt. %
	66.5-67.5	<0.5	47	19	140	1.0	11	15	22	4.8	0.7	0.05	2.6	0.05	6.5	0.37	6.6	0.10
	67.5-71	<0.5	24	14	100	0.6	10	11	21	6.2	0.3	0.02	2.8	0.06	6.7	0.39	3.8	0.04
	71-74	<0.5	23	14	89	0.5	9	10	22	6.3	0.6	0.04	2.6	0.05	6.8	0.39	3.2	0.03
	74-79	<0.5	47	15	155	0.9	15	17	28	8.7	0.8	0.04	3.2	0.19	7.2	0.39	4.6	0.03
	79-84	<0.5	38	15	110	0.4	9	13	27	6.3	0.7	0.02	3.0	0.05	7.3	0.43	3.7	0.04
	84-89	<0.5	26	16	93	0.4	8	11	24	4.5	0.6	0.03	2.5	0.03	6.6	0.39	2.5	0.03
	89-92.5	<0.5	29	15	98	0.5	9	11	20	5.4	0.6	0.02	2.6	0.06	7.0	0.39	2.7	0.03
	92.5-96	<0.5	29	13	99	0.4	9	10	21	5.5	0.6	0.03	2.9	0.06	7.3	0.40	2.5	0.03
	96-101	<0.5	30	15	96	0.5	8	10	20	6.4	0.6	0.02	2.8	0.06	7.3	0.37	2.7	0.03
	101-106	<0.5	32	16	105	0.7	12	12	20	6.6	0.7	0.03	3.2	0.10	8.2	0.42	2.4	0.03
	106-111	<0.5	29	17	94	0.4	11	10	18	6.6	0.6	0.03	3.0	0.09	7.6	0.39	2.3	0.02
	111-116	<0.5	34	19	105	0.4	10	13	22	5.3	0.8	0.03	3.1	0.09	7.4	0.40	2.6	0.03
	116-121	<0.5	34	13	105	0.2	10	13	22	5.6	0.7	0.05	3.1	0.07	7.7	0.42	2.7	0.02
	121-126	<0.5	28	14	96	0.3	8	10	18	4.9	0.7	0.03	3.0	0.05	7.5	0.39	2.4	0.02
	126-131	<0.5	30	14	100	0.6	11	11	19	9.8	0.7	0.03	3.4	0.10	8.2	0.41	2.0	0.02
	131-136	<0.5	27	15	88	1.2	10	11	18	6.0	0.7	0.02	3.0	0.10	7.5	0.37	2.2	0.02
	136-138	<0.5	28	16	87	1.1	13	12	17	9.7	0.7	0.03	3.4	0.22	7.6	0.38	2.9	0.02

Appendix 2 - ¹³⁷Cs GEOCHRONOLOGY

Introduction

¹³⁷Cs has been used extensively to estimate average post-1960s sediment accumulation rates in lakes and reservoirs (Ritchie and McHenry, 1980). The method is based on the well-established time-dependence of ¹³⁷Cs fallout ($t_{1/2} = 30.2y$) to water bodies from remote atmospheric (above-ground) testing of nuclear weapons. Often, a clear ¹³⁷Cs peak in a sediment core can be reliably associated with the occurrence of maximum deposition during the years 1963-1964. In favorable cases, additional minor peaks (e.g., 1959) in the depositional record may be identified (Callendar and Robbins, 1993). The onset of detectable ¹³⁷Cs deposition is normally ascribed to 1953±1y.

Idealized Loading of ¹³⁷Cs to Terrace Reservoir

Apparently, no ¹³⁷Cs fallout measurements have been made in or around the Terrace Reservoir area. However, an idealized deposition pattern is sufficient to characterize the historical record for the present study. For this purpose, a carefully constructed rate of deposition of ¹³⁷Cs deposition in the Great Lakes region, based on the HASL monitoring network will suffice (HASL, 1977; Robbins, 1986). Deposition in Terrace Reservoir will not differ significantly from this pattern insofar as the present use is concerned. If a more accurate atmospheric flux were required, it could be constructed using local precipitation data.

In the Terrace Reservoir system, the ratio of catchment to lake area is large (~350 times). Thus, the runoff of ¹³⁷Cs from the drainage basin to the reservoir is undoubtedly important and, in fact, is likely to dominate loadings to the catchment. Whereas complex models of the transport of soil-reactive tracers to catchments are available (e.g., Shukla, 1993), a simple first-order model suffices for the present case. If $S_C(t)$, in dpm cm⁻² of catchment, is the amount of ¹³⁷Cs stored on the catchment as a function of time, first-order mass balance requires that

$$dS_C/dt = 0.99F_a(t) - (\lambda + \lambda_r)S_C \quad (1)$$

where:

F_a = atmospheric ¹³⁷Cs fallout rate in dpm cm⁻² y⁻¹

λ = reciprocal lifetime of ¹³⁷Cs (0.69315/30.2y⁻¹)

λ_r = first order removal rate constant for ¹³⁷Cs from the basin

The 0.99 factor applied to the atmospheric flux (fallout rate) accounts for the observation that roughly 99% of the radionuclide is retained for long periods on catchments whereas a small but significant fraction (~1-2%) is transferred within a few months after deposition (e.g., Menzel, 1974). The total amount of the radionuclide transferred to the lake, F_l (dpm cm⁻² of lake y⁻¹), then consists of three components:

$$F_l(t) = F_a + 0.01F_a(A_C/A_l) + \lambda_r[(A_C/A_l)]S_C \quad (2)$$

where:

F_a = direct atmospheric transfer of ¹³⁷Cs to the reservoir surface

$0.01F_a(A_C/A_l)$ = rapid transfer of about 1% of the catchment flux of ¹³⁷Cs

$\lambda_r[(A_C/A_l)]S_C$ = slow erosional component of ¹³⁷Cs flux

A_C/A_l = catchment to reservoir area ratio

Values in the literature for λ_r generally are around 0.1 to 0.01%/y corresponding to ¹³⁷Cs residence times ($1/\lambda_r$) of 1,000 to 10,000y (Santschi, and others, 1988; Shukla, 1993). In general, the residence time increases with time (Scott, and others, 1985) reflecting decreasing mobility of transients such as ¹³⁷Cs due to increased binding to soils and resistance to erosion. The rapid component, F_r , consisting of the first two terms in Eq. 2, is dominated by catchment loading if the 1% fraction is at all representative. Since the catchment in the Terrace Reservoir system is large, roughly 3.5 (1% of 350) times as much ¹³⁷Cs arrives via stream inflow than from atmospheric deposition. Using a value of $\lambda_r = 0.05\%/y$, the total load of ¹³⁷Cs [$F_l(t)$; Eq 2] to the reservoir can be calculated (Fig. A2-1). The principal effect of the 'slow' component (see Eq 2) is to elevate the post-1960s ¹³⁷Cs loading which dominates the flux after 1970 (see the smooth lower curve in Fig. A2-1). This slow erosional component contributes considerably to the total load of ¹³⁷Cs entering the reservoir. According to this idealized model, roughly 18, 64, and 38dpm cm⁻² of atmospheric, fast, and slow catchment loads (15, 53, and 32%) respectively entered the lake between 1953/1954 and the time of core collection in 1994.

Idealized Sedimentary Profile of ^{137}Cs in Terrace Reservoir

Often, for a number of reasons, the time-dependence of the loading of ^{137}Cs to water bodies is not well-reflected in sediment core profiles. These include pre-depositional effects such as retention of ^{137}Cs in the water, particularly of deep lakes, or temporary storage in marginal deposits with subsequent resuspension and deposition at a receptor (coring) site as might occur during focusing. Both processes tend to integrate loads by combining inputs to the system over a range of times. Further, post-depositional processes such as physical or biological mixing of sediments, chemical diagenesis, or even core sectioning at finite intervals are inherently integrative. The overall effect of all these processes is to constrain the time resolution with which sediment records can be used to reconstruct system loads (Robbins, 1982; Miller and Heit, 1986). The profiles described by these authors can be described by a simple first-order model which, while not specifying the precise nature of the integrative process, treats the load to a catchment as being stored temporarily with a characteristic integration time, T_1 . The flux of ^{137}Cs to a receptor site, F_{sed} , is then given by:

$$dF_{\text{sed}} / dt = \lambda_1 F_1 - (\lambda + \lambda_1) F_{\text{sed}} \quad (3)$$

where:

$$\begin{aligned} F_{\text{sed}} &= \text{flux of } ^{137}\text{Cs} \text{ to a receptor site} \\ T_1 &= \text{characteristic integration time} \\ \lambda_1 &= 1.0/T_1 \end{aligned}$$

Using Eq 3, with a somewhat arbitrary integration time of 3y, and using time rather than depth for the horizontal scale, an idealized downcore ^{137}Cs profile can be generated (Fig. A2-1). The primary effect of the integration is to smooth out the monthly variations evident in the flux to the reservoir (Fig. A2-1). The difference between the flux to the reservoir and the sediment profile results from correcting the ^{137}Cs concentration for radioactive decay in the core (Fig. A2-1). This results because the radioactive decay of ^{137}Cs increases with depth in the core; for example, ^{137}Cs activity deposited at the onset of measurable deposition (~1953/1954) is now some 2.5 times less by the time the cores were collected in 1994.

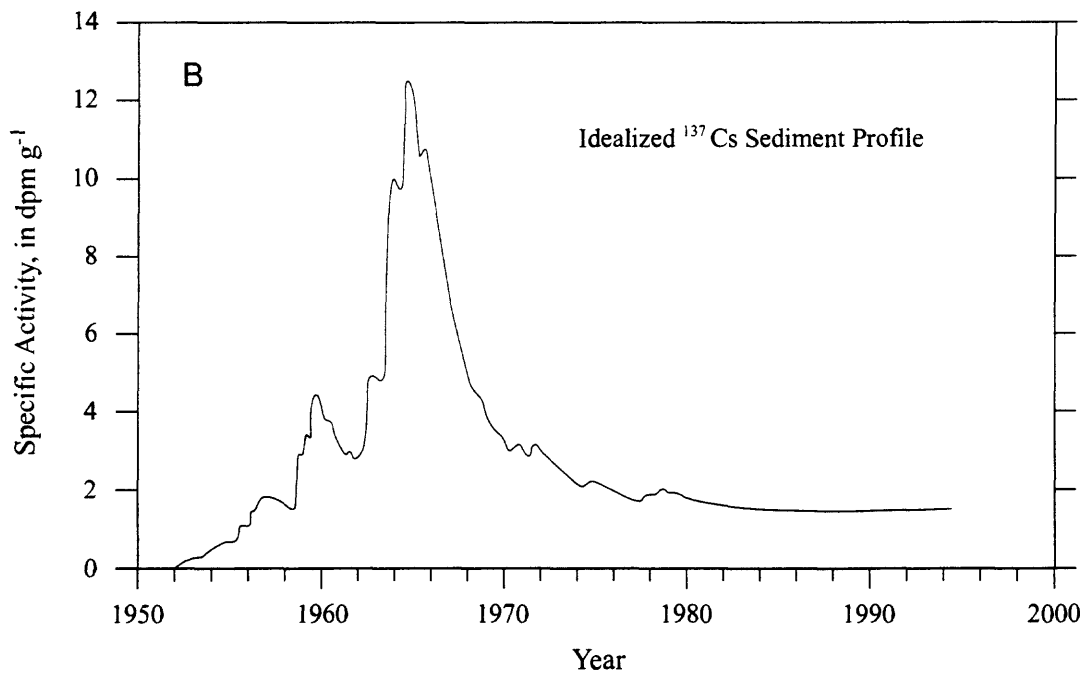
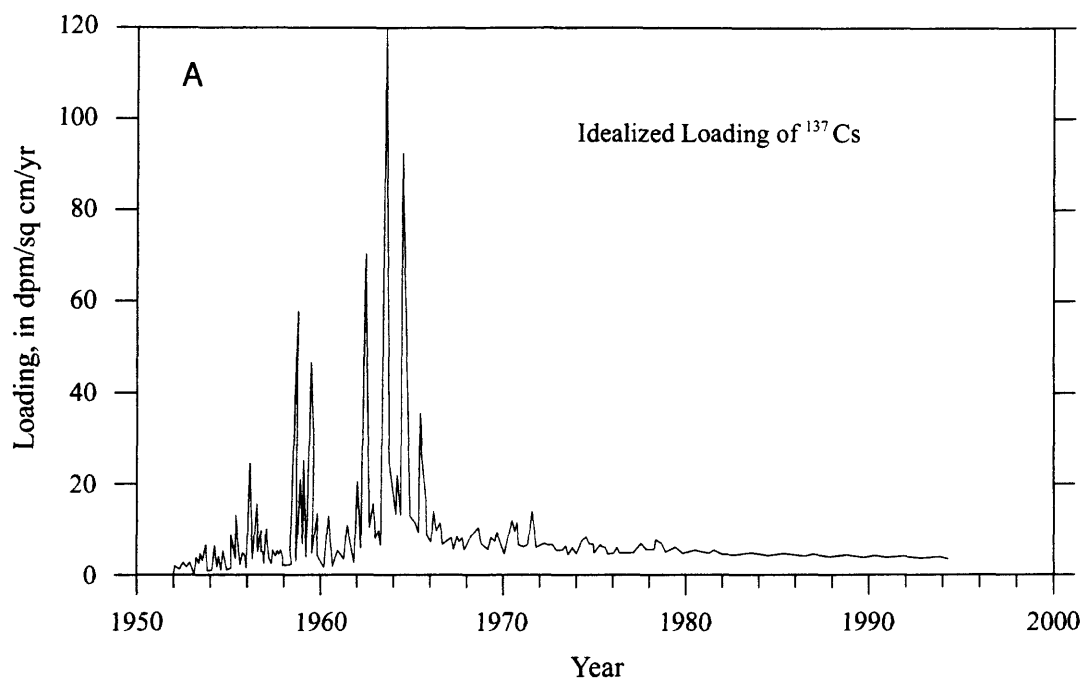


Figure A2.1. The upper graph (A) shows changes in the idealized ^{137}Cs loading, with time, to Terrace Reservoir, whereas the lower graph (B) shows a ^{137}Cs sedimentary profile assuming the delivery of the idealized ^{137}Cs loading depicted in the upper graph.

Appendix 3 - ²¹⁰Pb GEOCHRONOLOGY

Introduction

²¹⁰Pb has been used to determine rates of accumulation of recent sediments in a variety of aquatic environments (Robbins, 1978). ²¹⁰Pb is a member of the abbreviated uranium-series decay sequence: ²³⁸U (t_{1/2} = 4.5 x 10⁹ y) .. ²²⁶Ra (t_{1/2} = 1600 y) .. ²²²Rn (t_{1/2} = 4d) .. ²¹⁰Pb (t_{1/2} = 22.3 y) .. ²¹⁰Po (t_{1/2} = 138 d). ²²⁶Ra commonly is present in crustal materials; it decays to ²²²Rn which leaks into the atmosphere where it subsequently decays to ²¹⁰Pb. Thus, there is a relatively constant annual flux of this isotope to many water bodies as well as accumulation of ²¹⁰Pb in sediments. In addition to this 'excess' ²¹⁰Pb, there is a normal background contribution from *in situ* decay of Ra in sediment matrices. Decay of excess ²¹⁰Pb upon burial, can often be used to establish sediment chronologies extending back about 100y. In favorable cases, the ²¹⁰Pb method can provide information on changes in sedimentation rate with time. As with any dating technique, the method can produce spurious results if the distribution of excess ²¹⁰Pb has been altered by processes such as physical or biological mixing of sediments, or chemical diagenesis.

In general, if there is no post-depositional redistribution of sediment or radionuclides, the activity of excess ²¹⁰Pb is given by:

$$A_E = [F(t)/R(t)]e^{-\lambda t} \quad (1)$$

where:

- A_E = activity of excess ²¹⁰Pb
- F(t) = rate of supply of excess ²¹⁰Pb (dpm cm⁻² y⁻¹)
- R(t) = mass accumulation rate (g cm⁻² y⁻²)
- t = time
- λ = decay constant for ²¹⁰Pb

In turn, it can be shown that the age-depth relation for a given activity of excess ²¹⁰Pb is given by

$$g = \int_0^t R(t)dt \quad (2)$$

where:

- g = 'depth' as the cumulative weight of dry sediment (g cm⁻²)
- R(t) = mass accumulation rate (g cm⁻² y⁻²)

Since R(t) and F(t) can vary with time, an excess ²¹⁰Pb distribution alone, can not provide a unique sediment chronology. The time dependence of F or R must be independently specified. Common approaches include the assumption of a constant F, a constant R, or a constant ratio of F to R (Robbins and Herche, 1993). None of these approaches are likely to be entirely satisfactory in Terrace Reservoir since both the rate of supply of excess ²¹⁰Pb [F(t)] and the mass sedimentation rate [R(t)] have probably varied significantly in this system. Also, there is no evidence to suggest that the ratio F/R has been invariant. However, for purposes of comparison with the measured distribution of ²¹⁰Pb in V-4, a theoretical linear accumulation rate profile was calculated assuming a constant ratio of F/R. Under such conditions, it can be shown that:

$$A_E = A_0 e^{-\lambda z/w} \quad (3)$$

- where A_E = activity of excess ²¹⁰Pb
- A₀ = (F/R) at the time of deposition (dpm g⁻¹)
- λ = decay constant for ²¹⁰Pb
- z = sediment depth (cm)
- w = constant linear accumulation rate (cm y⁻¹)

For purposes of this calculation, compaction is considered insignificant in this core.